Mesoscopic transport in magnetically contacted quantum dots

Jesper Qvist Thomassen

Cand. Scient. Thesis
Ørsted laboratory, NBIfAFG
University of Copenhagen

Supervisor: Karsten Flensberg

20th August 2003

Abstract

Mesoscopic transport in magnetically contacted quantum dots is an investigation of the spin transport phenomena in quantum dots which are connected by magnetic contacts. Formulas for the electric current through the dot and the spin torque on the quantum dot are derived using real time Green's functions. The formulas are valid for arbitrary magnetizations of the two leads and the quantum dot.

Two models for the quantum dot are derived and used to examine the coherent and strongly correlated transport regimes. The two models are the non-interacting model and the constant Coulomb interaction model. The first is solved exact while the other is solved in the strong Coulomb limit.

The current through two configurations of the contacts is found in two transport regimes. The configurations are the ones where the magnetizations of the contacts are either parallel or anti-parallel. In both configurations the magnetization of the quantum dot is arbitrary. A resonance is found in the coherent regime. This resonance vanishes in the correlated regime due to the blocking of the current through one of the quantum dot levels because of the strong Coulomb interaction. These effects are shown to lead to negative magneto-resistance.

Acknowledgements

I owe great thanks to my supervisor Karsten Flensberg. He has provided encouragement and insight. Especially his insistence to keep things simple has been a great learning experience.

I will also thank Line P. Jensen, Thomas S. Jespersen, Jan-Erik Revsbech and my father Jens Q. Thomassen for their comments during the final stages finalizing my thesis.

Finally I would like to thank the University for founding of my visit to the University of Cornell to visit Karsten Flensberg for guidance and comments to the development of the theory in my thesis.

Contents

CHAPTER 1

Introduction

In resent years a lot of research has been put into the control of the electrons spin degree of freedom. Many of the systems researched are low dimensional systems. When Karsten and I started this project our aim were on charge and spin transport in one dimensional electron systems. This lead to the study of zero dimensional systems - quantum dots, which we realized were not well understood and rich in interesting phenomena and became the focus of this work.

Mesoscopic transport through a magnetically connected quantum dot connects a wide variety of fields in solid state physics. The purpose of this chapter is to escort the reader on a quick theoretical and experimental tour through the subjects of quantum dots, Coulomb blockade and spin transport. These fields developed in the last fifteen years with spin transport as the most resent and fastest development. In the last section, the work presented in this thesis will be put into perspective.

1.1 Mesoscopic systems

Mesoscopic physics is the description of the nature in the region between the macroscopic - classic physics and the microscopic - atomic physics. The length scales are in between a few nanometers (10^{-9}m) to about a micron (10^{-6}m) a regime where the sample is larger than an atom but smaller than the energy relaxation length. Transport through these systems combines physics on many length scales and results in very interesting phenomena. For example in transport through narrow wires the conductance is quantized. The field of transport through mesoscopic systems is huge and we will here concentrate on the electric and spin currents through quantum dots.

1.2 Quantum dots

In the late 1980's it became possible to make structures smaller than 1μm in semiconductor materials. This lead to the first experiments with quantum dots [25]. Quantum dots are pure quantum mechanical objects and are also known as quantum wells or artificial atoms. They can be made in semiconductor materials using nanoscale lithography techniques e.g. planar confinement of the electrical carriers in a 2DEG (quasi-two-dimensional electron gas) in a GaAs/AlGaAs heterostructure. Mesoscopic molecules like carbon nanotubes behave like quantum dots at low temperatures. This is due to the tunneling contact usually formed with the connecting lead and that the thermal energy becomes less than the energy needed to add an extra unit charge to the tube. This means that there is a wide variety of experimental realizations where the theory of quantum dots can be used.

The energy spectrum of a quantum dot is discrete. The level spacing and degeneracy depends on the shape of the confinement and external applied fields. Here we will not go into a discussion of different spectra but [6] or [7] are fine references. The Hamiltonian of an quantum dot in a magnetic field will be discussed in section 2.1.3.

There are different methods to contact the quantum dot. In some experimental setups quantum point contacts are used (semiconductor devices) and in others metallic contacts are utilized (semiconductor-molecular systems) but in both kinds the coupling is described by tunnelling through a potential barrier[1].

The nature of the contacts range from metallic- to ferromagnetic alloys and recently ferromagnetic semiconductors. This will be discussed in more detail in section 1.3.1. There is a lot of different models describing this kind of system some with more luck than others. The Hamiltonian we are using was first introduced by P. W. Anderson [2] to describe magnetic atoms in a metal - one contact to one atom. We will not use Anderson's methods to calculate the quantities but will instead use a method inspired by Meir and Wingreen [23]. Here the non-equilibrium Keldysh formalism is used to derive a Landauer like formula for transport through a region with interacting electrons. Their main result is very similar to equation 4.16 in chapter 4. In the limit with a non interacting quantum dot the formula reduces to the two terminal Landauer formula. Their results have been extended to the time dependent case [12].

[1] Semiconductor quantum dots can be contacted without using tunneling barriers, but in order to obtain a high polarization with metallic contacts a tunneling barrier have to be used [9].

1.2.1 Coulomb blockade

One of the main characteristics of a quantum dot is the Coulomb blockade. When an electron tunnel into the quantum dot it introduces a change in the electrostatic potential of the dot. This can at low temperatures give a gap in the energy spectrum at the Fermi levels of the contacts. This phenomena is called the Coulomb blockade. One of the main features is the occurrence of periodic oscillations in the conductance as a function of the gate voltage [25]. The oscillations are due to the discrete energy spectrum of the dot. When the temperature decreases the broadening of the levels also decrease. This leads to the energy gaps. This means that by sweeping the gate voltage one can obtain information of the energy spectrum of the dot[2]. The Coulomb blockade is also used as a diagnostic tool to determine the isolation of a region in a semiconductor structure.

Many of the features of the Coulomb blockade can be understood with a simple tunneling model using only single electron quantum- and statistical mechanics [3]. The method used here involves many-particle physics and it is described in length in [24], where an Anderson model with Coulomb interaction in the quantum dot is used. This is discussed in chapter 6.

1.3 Spin transport

Recently it has been made possible to use the spin degree of freedom of electrons in devices instead of only the electronic properties. The first example was the giant magneto-resistance (GMR). Now a multi million dollar business in modern hard drive read/write heads. The control of the spin is possible through its coupling to a magnetic field.

The effects of the spin degree of freedom can be found when currents are passed through structures containing ferromagnetic materials thus creating spin polarized currents.

1.3.1 Ferromagnetic leads

When experimentalists wants to examine the spin transport properties of a structure, they exchanges the usual metallic contacts with ferromagnetic materials. The resent discovery of ferromagnetic semiconductor materials have reference helped in building pure semiconductor structures instead of introducing metals into the structure. Before going into the resent experimental results let us delve on the differences between the metallic and ferromagnetic contacts and shortly review the previous theoretical works.

[2]Resently measurements of spin transitions in quantum dots have been reported [30].

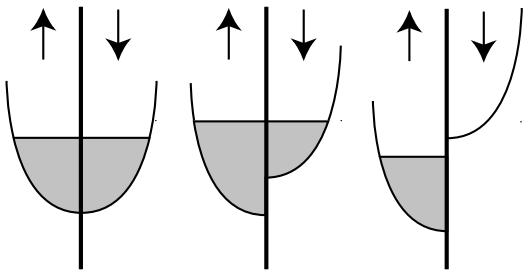

Figure 1.1: The three figures show the different fillings of the spin bands. The bands are filled to the Fermi level of the material. To the left is a normal metal. Here there are equal amounts of spin up as spin down electrons. The middle is a ferromagnet. It has a different amount of up and down electrons - a finite magnetization. Furthermore there are a larger amount of up electrons at the Fermi level. The electrons at the Fermi level are primarily the one contributing to transport processes. The right figure shows a fully polarized ferromagnet such a material is also known as a half metal. In this material the electrons have only one kind of spin.

In figure 1.1 the filling of the conduction bands for metals and ferromagnets are shown. In a metal the energy states are spin degenerate and therefore the filling of the spin up and spin down bands are identical. In a ferromagnet this degeneracy is lifted and spin states have a different filling. When a current is sent through a ferromagnet the charge carriers which leave the magnet will depend on the direction of the magnetization. This spin polarized current can then be injected into another material.

Consider a simple setup with a source and drain connected by a tunneling barrier. When a ferromagnet is used as a source contact the electrons available for the tunneling will predominately be spin up. This should match with the structure of the drain for the full number of injected carriers to transfer. If the structures are different some of the injected carriers scatter and a drop in the current occurs. If the drain is a magnetized anti-parallel to the source and both are fully polarized the current vanishes completely. This was first proposed by Julliére [15] and further investigated by J.C. Slonczewski [34]. This effect is refereed to as a spin valve and illustrated in figure 1.2.

Later a quantum dot (and tunneling barriers) has been added to the structure leading the papers [18] [33] [38][35]. These papers all treat the same structure but focus on different phenomena and use different methods. König and Martinek [18] considers a HM-QD-HM[3] structure (the QD has one spin degenerate level and they find the linear conductance and spin accumulation using density matrices and rate equations. They find that the accumulated

[3]HM stands for half metal. This is a metal where the conducting electrons all have the same spin. QD means a quantum dot.

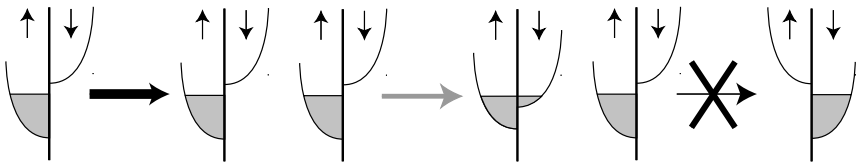

Figure 1.2: The three figures illustrate the spin valve effect. In the left figure the half metal have the same amount of electrons at the Fermi level. In the middle figure the left is a half metal while the right is a ferromagnet. A current can flow through these materials because the ferromagnet has a finite Fermi surface for the half metal's up electrons. In the third figure no current can run because the right half metal has no Fermi surface where it can put the up electron from the left half metal.

spin is along the y-axis (defined as $\frac{\hat{n_L}-\hat{n_R}}{|\hat{n_L}-\hat{n_R}|}$) with no charging energy (no Coulomb interaction) but turns into the xz-plane when the charging energy is turned on (the z-axis is diagonal to the directions of the leads). The conductance shows the magnetic spin valve effect with a dependence on the energy difference between the Fermi sea and level energy.

The three other papers use the same approach as in this thesis. The first two [33][38] considers a FM-QD-FM system with the magnetizations of the leads at an angle θ. Their result is similar to equation . They focus on the behavior of the Kondo peak and the non-linear conductance. The Kondo effect is due to the formation of a many-body state involving the localized spin on the dot and a coherent state of the conductance electrons. The effect should vanish if the spin states have a strong splitting. We will not go into a deeper discussion of this because we will not consider Kondo physics in this thesis. Sergueev et.al. also see a magnetic spin valve effect but do not find any simple analytical expression. In [35] the FM-QD-FM[4] is only considered for the parallel and anti-parallel configurations with Hartree-Fock approximation of the Coulomb interaction with an extra spin-flip term. Furthermore they consider the noise of the system. They find that the spin flip tends to remove the spin valve effect of the different alignment of the leads for both the current and the noise.

The physical idea of the spin torque is based on the article by Waintal et.al. [36] where they calculate the current induced spin torques in metallic magnetic multilayers. The spin torque is the torque exerted on the magnetization of the region by a spin polarized current passing through the region. This effect is a mechanism separate from the effects due to the magnetic field. At sufficient high current densities it is believed that the spin torque can alter the magnetization state of the region.

[4]FM means a ferromagnet.

1.3.2 Experiments

Spin injection into a normal metal was achieved by Johnson and Silisbee [14]. Later interest was raised concerning injection into semiconductors because of the proposal made by Datta and Das for a spin-field effect transistor [5]. This proved to be complicated. The problems could be solved by introducing tunneling barriers [9] or using a new kind of dilute magnetic semiconductors [8] [29].

Several groups have made experiments with spin injection into carbon nanotubes The experiments were first done with multi-wall nanotubes and later for single walled nanotubes[5]. For a review of experiments see [13]. Recently experiments have been made at the Ørsted laboratory[6] with single-walled nanotubes connected to metallic Fe or dilute magnetic semiconductor contacts [13]. Common for these experiments are that they show the magnetic spin valve effect but with a variety of strength and sign. In particular a huge magneto resistance is observed at low temperatures which could be related to a resonance phenomena.

Magneto-resistance is a broad term for an electric resistance dependent on the magnetic field. Different kinds of phenomena give rise to a magneto-resistance e.g. anisotropic magneto-resistance originating from the coupling between the carrier spin and the orbital motion. When magneto-resistance is used about nanotube measurements is it usually meaning the increase in resistance when comparing setups with anti-parallel and parallel alignment of the magnetizations of the contacts. Further measurements on systems with one ferro magnetic contact and one metallic contact also show a magneto resistance. This cannot be explained by the Julliére model. Other measurements have found a less outspoken magneto-resistance effect (for multiwalled tupes) and the separation of spin and charge in a Luttinger Liquid is given as a proposed explanation [11] .

At the moment it is unclear which is the relevant phenomena in these systems. Therefore it is important to find out to what extent the different proposals can account for the observations. The aim of the work in this thesis is to clarify which contributions resonance phenomena can contribute to the magneto-resistance.

1.4 This thesis

The work in this thesis is focused on building a model for transport of electric carriers and spin through a FM-QD-FM system. The methods used are as

[5] The difference between multi- and single-walled is the number of cylindrical carbon shells put into each other. In single-walled the tube consists only of a single shell while in multi-walled the tube have several shells.

[6] Niels Bohr Institute for Astronomy, Physics and Geophysics.

already mentioned based on the model of Meir, Wingreen and Lee [24] with the idea regarding the spin torque from Waintal et.al. [36]. The result is rather general and is applicative for an arbitrary configuration for the ferromagnetic leads and the quantum dot. Further the result is valid for a finite bias voltage applied to the system. Though the linear response regime is the main focus of the analysis.

1.4.1 Contents of the chapters

The thesis consists of three parts. First a general formula is derived for the electric current that runs through the system and the spin torque on the quantum dot. This is done in chapters 2 to 4. Then two models of a non-interacting dot and a Coulomb interacting dot are discussed in chapters 5 and 6. The findings from the first two parts are combined and the results are applied to a simple configuration of the contacts and quantum dot in chapter 7. In the following the contents of the chapters are outlined.

Chapter 2: Transport model

The model is presented and the form of the Hamiltonians are discussed. Then the formulas for the electric current and spin torques are derived from first principles. All formulas depend on the current Green's function which needs to be determined.

Chapter 3: Non-equilibrium quantum field theory

A review of the non-equilibrium quantum field theory is given with emphasis on the Keldysh formulation and Langreth's rules of analytic continuation.

Chapter 4: General trace formula (GTF)

In the light of the previous chapter the lesser current Green's function is decomposed into a lead[7] and a dot Green's function and the rules of analytical continuation are used. After some integration the general trace formula for the current and spin torques are found. Lastly the configurations where a proportionate coupling is possible are found.

Chapter 5: Non-interacting quantum dot

The first model for the structure of the quantum dot is presented here. It contains only the coupling between the leads and the quantum dot. The relevant quantities are found using equation of motion theory.

[7] Through the thesis we will not distinguish between a lead and a contact. Usually we will use contact when we discuss the physical region and lead when we are referring to the theoretic structure of the contact.

Chapter 6: Quantum dot with Coulomb blockade

Here the model from the previous chapter is expanded to include Coulomb interactions. The closure of the equations is discussed and a simple closure is used. An approximation scheme is introduced to find the lesser self-energy.

Chapter 7: The current through the quantum dot

The results from the previous chapters are combined and used on a simple configuration of the magnetizations. The linear response scheme is discussed. The electric current is found for various values of important parameters e.g. the polarization of the leads, the level placement and the strength of the Coulomb interaction.

Chapter 8: Summary and outlook

The findings of the chapters are discussed and conclusions are drawn. Future investigations are discussed.

Appendix

In the appendix simple calculations have been put for easy reference. This is usually calculations which shed no new light on the problematics or are simple mathematical derivations. The appendix also contains a list of symbols.

CHAPTER 2

Transport model

The theory involved in the description of the transport of charge and spin through an interacting mesoscopic system with non-collinear magnetic contacts is a combination of different fields in condensed matter physics. The transport equations will be developed from first principles and are applicable to a large group of mesoscopic systems.

The reader should have a good knowledge of quantum mechanics and be familiar with second quantization. For an introduction into second quantization see [4]. In this thesis $\hbar$ and k_B are set to 1 unless otherwise stated. This means that frequencies and temperatures are measured in units of energy.

In the first sections the Hamiltonian of the system will be discussed in detail with emphasis on the coupling of the different regions, followed by derivation of the transport formulas.

2.1 The Hamiltonian of system

The system consists of three spatially distinct regions. A left and a right (ferro-)magnetic lead and a middle region. By a lead is meant the theoretical model of the contact. The leads are viewed as magnetic reservoirs[1] with different (electro-)chemical potentials. The system will try to equalize this potential difference with a current running through the system. The

[1] The contacts are considered macroscopic and therefore the depletion electrons with the same spin is neglected.

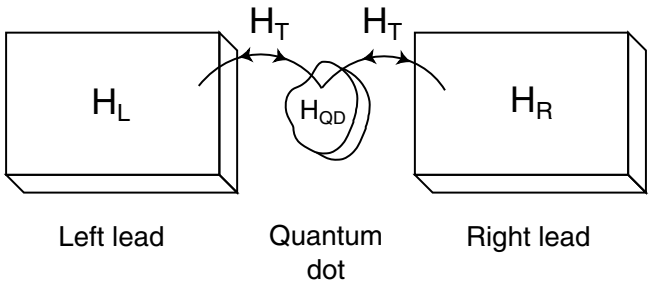

Figure 2.1: The figure illustrated the Hamiltonians of the system. The three regions (left and right contact and the quantum dot) have each their own Hamiltonian which only contains information about the respective region. Furthermore the coupling between the regions are described by a separate Hamiltonian.

derivations in this chapter do not require a detailed description of the middle region[2] but throughout the thesis the middle region will be modeled as a quantum dot and will be referred to as such.

The contacts are considered non-collinear which means that the magnetizations are not necessarily parallel or anti-parallel. Furthermore, it is assumed that the quantum dot is spin split. This spin splitting could be due to the Zeeman splitting of the energy levels due to an external magnetic field. The different magnetizations of the regions means that each region has a preferred spin basis. This preferred spin basis of the region will generally be different and a description of the change of spin basis has to be included in the theory.

The Hamiltonian describing the system consists of four parts

$$H = H_L + H_R + H_{QD} + H_T \tag{2.1}$$

two describing the leads (H_R, H_L), one describing the quantum dot (H_{QD}) and finally one describing the coupling between the leads and the quantum dot (H_T). The Hamiltonian is illustrated in figure 2.1.

2.1.1 Spinors

The description separates the spin variables from the other quantum numbers. This separation allows us to treat the spin in its own Hilbert space disjoint from the other variables combined spaces. The spin variables are treated in an abstract two-dimensional complex vector space. The Hamiltonian of the system can be expressed by using a compact spinor formalism. A

[2] The derivations presented in this chapter only need the existence of a complete set of fermion field operators describing the middle region [12].

spinor is a two component object which transform into a spinor again under $SU(2)$ transformations [19]. Using this formalism the spinor annihilation (creation) operator looks like

$$\vec{a}_k^{(\dagger)} = \begin{pmatrix} a_{k\uparrow}^{(\dagger)} \\ a_{k\downarrow}^{(\dagger)} \end{pmatrix} \tag{2.2}$$

where $a_{k\uparrow}^{(\dagger)}$ is a annihilation (creation) operator with spin-up and k is a collection of the other quantum numbers needed to fully describe the state. Using this spinor formalism allows us to use vector operations like the dot and matrix product on the spinors to formulate the theory. The states of the system are the normal many particle states [4]

$$a_{k\uparrow}^\dagger |n_{k\uparrow}>= |n_{k\uparrow}+1> \quad a_{k\uparrow}|n_{k\uparrow}>= |n_{k\uparrow}-1> \tag{2.3}$$

2.1.2 The lead Hamiltonians

The form of the Hamiltonians for the two leads are identical. The leads are assumed non-interacting and therefore their Hamiltonians consists of two parts - a kinetic and a magnetic.

$$H_\alpha = \sum_k \epsilon_k^0 \vec{c}_{k\alpha}^\dagger \cdot \vec{c}_{k\alpha} + \sum_k \vec{c}_{k\alpha}^\dagger \cdot \left(\vec{\bar{\sigma}} \cdot \vec{M}_{k\alpha}\right) \vec{c}_{k\alpha} \tag{2.4}$$

Where $\vec{c}_{k\alpha}^\dagger$ is a spinor creation operator for the alpha lead. $\vec{\bar{\sigma}}$ is the Pauli matrix vector consisting of the three Pauli matrices and $\vec{M}_{k\alpha}$ contains the size and direction of the magnetization of the lead. The bar above the σ is the notation for a 2-by-2 spin space matrix. ϵ_0 is the free single particle energy.

The kinetic term is independent of the spin and is therefore diagonal in arbitrary spin bases. In this form, the choice of basis for the operators is arbitrary and the Hamiltonian is not necessarily diagonal in spin space. Inserting the unitary rotation matrix (U) which diagonalizes the magnetization matrix, the operators are rotated into the diagonal basis. The diagonalized Hamiltonian has the form

$$H_\alpha = H_{kin} + \sum_k \left(\vec{c}_{k\alpha}^\dagger U^\dagger\right) \cdot \left(U(\vec{\bar{\sigma}} \cdot \vec{M}_{k\alpha}) U^\dagger\right) \left(U \vec{c}_{k\alpha}\right) = \sum_k \vec{a}_{k\alpha}^\dagger \cdot \bar{\mathcal{E}}_{k\alpha} \vec{a}_{k\alpha} \tag{2.5}$$

where $\vec{a}_{k\alpha}^\dagger$ is the spinor creation operator in the diagonal basis and $\mathcal{E}_{k\alpha,\mu\mu'} = \epsilon_k^0 \delta_{\mu\mu'} + \sigma_{z,\mu\mu'} M_{k,\mu\mu}$ is a diagonal energy matrix given as the sum of the kinetic term and the diagonalized magnetization matrix.

The ϵ_k^0 is measured from the chemical potential of the respective lead. The finite voltage bias of the contacts is put into the model through a difference between the left and right chemical potential.

Why have we spend that many lines on the diagonalization of this Hamiltonian? We could have written the diagonal Hamiltonian and neglected the discussion about the change of basis. The reason for this discussion is to stress the importance of the chosen spin basis. The fact that we have chosen the spin basis where the magnetic parts of the Hamiltonians are diagonal has the consequence that all the information about the relative directions of the magnetizations of the regions are contained in the coupling Hamiltonian.

2.1.3 The quantum dot Hamiltonian

The quantum dot Hamiltonian consists of two parts. First a diagonal term containing kinetic and magnetization parts like the lead Hamiltonians and secondly an interaction part. The operators are expressed in the diagonal spin basis.

$$H_{QD} = \sum_n \vec{d}_n^\dagger \cdot \bar{\mathcal{E}}_n \vec{d}_n + H_{int} \tag{2.6}$$

The n-index is a collection of quantum numbers needed to fully describe the energy spectrum of the quantum dot - again except for the spin. The energy matrix $\bar{\mathcal{E}}_n$ consists of a term dependent on the geometry of the dot and a magnetic term. The splitting is assumed to come from the Zeeman effect which is due to an external magnetic field. The magnetic field is not put directly into the model but is hidden in the difference of the energies of states with the same n-quantum numbers. The description is valid for all magnetic fields. The dependence on the external magnetic field could easily be included in the model. This would mean a dependence of both the free level energies and the Zeeman energy on the field strength.

2.1.4 The coupling Hamiltonian

The coupling Hamiltonian describes the processes relating to the tunneling between the contacts and the quantum dot. The Hamiltonian has the form

$$H_T = \sum_{\substack{nk \\ \alpha=\{L,R\}}} \vec{a}_{k\alpha}^\dagger \cdot \bar{V}_{k\alpha,n} \vec{d}_n + H.c. \quad \left(= \sum_{\substack{nk\alpha \\ \sigma\sigma'}} a_{k\alpha\sigma}^\dagger V_{k\alpha\sigma,n\sigma'} d_{n\sigma'} + H.c. \right) \tag{2.7}$$

The lead and dot operators are expressed in different spin bases and the change of basis is contained in the coupling matrix $\bar{V}_{n,k\alpha}$. This means the coupling matrix contains all the information about the tunneling between the regions plus the change of spin basis. The term explicit written in the equation describes the process where an electron moves from the quantum dot to the α-lead. The Hermitian conjugate of this term ($H.C.$) describes the inverse process.

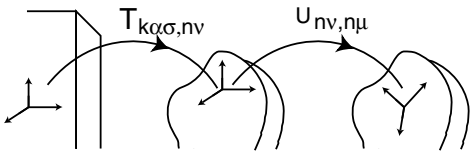

Figure 2.2: The coupling visualized. Read from left to right an electron tunnel into the dot (amplitude T) and changes basis (amplitude U). If the figure is read from right to left the opposite happens.

Coupling amplitudes

The entries of the coupling matrix are given by the overlap of the states in the respective lead and the states of the quantum dot.

$$V_{k\alpha\nu,n\sigma} = \langle k\alpha\nu|H_T|n\sigma\rangle = \sum_{m\sigma'}\langle k\alpha\nu|H_T|m\sigma'\rangle\langle m\sigma'|n\sigma\rangle = \sum_{m\sigma'} T_{k\alpha\nu;m\sigma'}R_{m\sigma',n\sigma} \tag{2.8}$$

where a complete set of states is inserted to factorize the coupling matrix into a tunneling ($T_{k\alpha,m\sigma'} = \langle k\alpha\nu|H_T|m\sigma'\rangle$) and a rotation part ($R_{m\sigma',n\sigma} = \langle m\sigma'|n\sigma\rangle$).

This allows a simple interpretation of the coupling which is illustrated in figure 2.2. If we consider the Hermitian conjugate process then a tunneling matrix describes the coupling between the states in the lead and the states in the quantum dot. All these states are in the same spin basis. The change of basis is made by a rotation matrix which expresses the dot-states in the lead basis in terms of the diagonal-dot-basis.

The elements of the tunneling matrix can be found using a tunneling-through-a-potential-barrier model. The tunneling matrix will later (section 4.3) be scaled into a matrix containing dimensionless parameters. Until then the matrix will have the following diagonal structure. We assume it to be diagonal because

we do not allow spin flips in the tunneling.

$$\bar{T}_{k\alpha,n} = \begin{bmatrix} t_{k\alpha\uparrow,n\uparrow} & 0 \\ 0 & t_{k\alpha\downarrow,n\downarrow} \end{bmatrix} \tag{2.9}$$

The rotation matrix is diagonal in n-space and has the form of equation 2.12 in spin space

$$\bar{R}_{m,n} = \delta_{mn}\bar{U} \tag{2.10}$$

These assumptions gives the coupling matrix the form

$$\bar{V}_{k\alpha,n} = \bar{T}_{k\alpha,n}\bar{U} \tag{2.11}$$

2.1.5 Change of basis

The non-collinearity of the system introduces spin flips when the electrons tunnel from one region to the other due to the different diagonal bases. The rotation matrix which describe the change of basis for the spinors is found in the literature ([19],[26]).

$$\bar{U}(\phi,\hat{n}) = \exp\left(-\frac{i}{2}\phi\hat{n}\cdot\vec{\sigma}\right) \tag{2.12}$$

where ϕ is the angle of rotation, $\hat{n}$ is the axis of rotation and $\vec{\sigma}$ is vector consisting of the Pauli spin matrices. The rotation matrix from the literature is from first quantization theory. It can be shown that this rotation matrix is the same as the one which transform the creation spinor. We therefore have the following transformation equations for the spinor operators

$$c^{\dagger}_{k\uparrow} = a^{\dagger}_{k\uparrow}\bar{U} \tag{2.13}$$

$$c_{k\uparrow} = \bar{U}^{\dagger}a_{k\uparrow} \tag{2.14}$$

These transformations will be used in section 2.1.4 to make a model of the tunnelling coupling between two regions described by operators in different spin-bases.

The rotation matrix

The model contains three magnetization directions. To describe their position to each other, we need three angles. The model is independent on how the coordinate system is chosen but the wisest is of cause to choose a coordinatesystem in which the transformation matrices are simple. If the magnetization of the quantum dot is chosen as the z-axis and the x-axis is chosen arbitrary, then the left and right lead magnetizations will be transformed by first a rotation about the z-axis until they lie in the xz-plane and secondly by a rotation about the y-axis. The angles are shown in figure 2.3. By defining the rotations this way four angles have been used, but it will be seen later that the formulas will depend on both of the polar angles (θ and ψ) but only on the difference of the azimutal angles (the ζ and ϕ angles). The polar angles are defined in the interval $[0,\pi]$ while the azimutal angles are defind in the interval $[0,2\pi]$

The transformation matrices describing the above rotations can be calculated directly from (2.12) or found in Landau and Lifshitz [19].

$$\begin{aligned} U_L(\theta,\zeta) =& U(-\theta,\hat{y})U(-\zeta,\hat{z}) = \begin{bmatrix} \cos\frac{\theta}{2} & -\sin\frac{\theta}{2} \\ \sin\frac{\theta}{2} & \cos\frac{\theta}{2} \end{bmatrix}\begin{bmatrix} e^{-i\frac{\zeta}{2}} & 0 \\ 0 & e^{i\frac{\zeta}{2}} \end{bmatrix} \\ =& \begin{bmatrix} \cos\frac{\theta}{2}e^{-i\frac{\zeta}{2}} & -\sin\frac{\theta}{2}e^{i\frac{\zeta}{2}} \\ \sin\frac{\theta}{2}e^{-i\frac{\zeta}{2}} & \cos\frac{\theta}{2}e^{i\frac{\zeta}{2}} \end{bmatrix} \end{aligned} \tag{2.15}$$

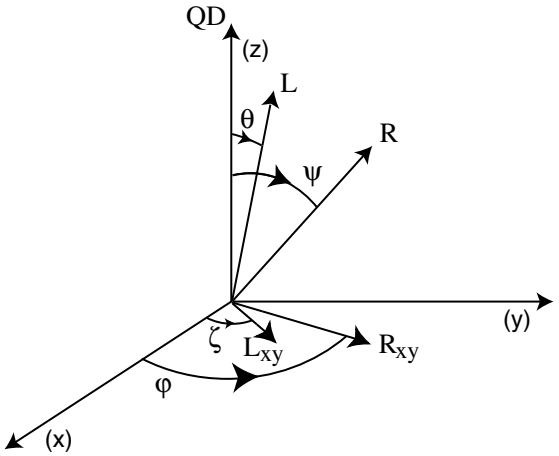

Figure 2.3: The four angles of rotation are shown. QD, R and L names the directions of the quantum dot, right lead and left lead magnetizations respectively.

The right transformation matrix is identical to the left transformation matrix except for ψ instead of θ and ϕ instead of ζ. These matrices are useable for an arbitrary configuration of the magnetizations but in the systems which are presented later in this thesis the matrices will simplify.

2.2 Transport formula

The transport through the quantum dot is now going to be derived in the general case by examining the time derivative of the occupation number operator and spin operators. These deriviations can be made more formal by using the similarity of the operators.

The system is assumed to be in steady state. Therefore the current density is independent of time. The continuity equation for the electric carriers is valid

$$\vec{\nabla} \cdot \vec{J} + \frac{\partial \rho}{\partial t} = 0 \tag{2.16}$$

The current density term is zero and we want to determine the current through a yz-cross section. This gives that $\nabla_x J_x = 0$. This independence on the position of the cross section will be used in the determination of the current. The spin is not a conserved quantity in equlibrium and we can therefore not apply the same considerations there.

2.2.1 The general notation

The operators of the quantities (electric current and torque) we seek to find have a close formal connection. Both kind of operators will be calculated as time derivatives of the occupation number (N) and spin operators ($\vec{s}$) respectively .

$$N = \sum_{\nu} \vec{a}_{\nu}^{\dagger} \cdot \vec{a}_{\nu} \qquad \vec{s} = \frac{\hbar}{2} \sum_{\nu} \vec{a}_{\nu}^{\dagger} \cdot \vec{\sigma} \vec{a}_{\nu}$$

These operators can formally be expressed by one operator. The spin-occupation operator which has four components is defined as

$$\bar{N}_i = \sum_{k} \vec{a}_k^{\dagger} \otimes \bar{\sigma}_i \vec{a}_k \qquad \left(N_{i,\eta\eta'} = \sum_{k\gamma} a_{k\eta}^{\dagger} \sigma_{i,\eta'\gamma} a_{\gamma} \right)$$

Where $\otimes$ is a matrix product and $\bar{\sigma}_i$ is defined as

$$\bar{\sigma}_0 = \mathbb{I} \, , \; \bar{\sigma}_1 = \sigma_x \, , \; \bar{\sigma}_2 = \sigma_y \, , \; \bar{\sigma}_3 = \sigma_z$$

With this definition the four operators are written as the trace of the four components of the spin occupation operator

$$\begin{aligned} N &= \mathrm{Tr}_s[\bar{N}_0] \\ s_x &= \mathrm{Tr}_s[\bar{N}_1] \\ s_y &= \mathrm{Tr}_s[\bar{N}_2] \\ s_z &= \mathrm{Tr}_s[\bar{N}_3] \end{aligned} \tag{2.17}$$

Here Tr_s means a trace in spin space defined as $\mathrm{Tr}_s[\bar{A}] = \sum_{\mu} A_{\mu\mu}$.

2.2.2 Time derivative of spin-occupation matrix

The electric current and QD-torque will be calculated in different regions. As already mentioned the electric current could be calculated in an arbitrary cross section because of current conservation and the condition of steady state. The occupation of the quantum dot is constant due to steady state and the time derivative would therefore be zero. This means that the electric current can be calculated in the leads. The QD-torque needs to be calculated in the quantum dot because the spin is not a conserved quantity.

The spin occupation current is the trace of the time derivative of the spin-occupation matrix.

$$\langle J_i^{\rho} \rangle = \mathrm{Tr}_s \left[\frac{d}{dt} \left(\langle \bar{N}_i^{\rho} \rangle \right) \right] = \frac{i}{\hbar} \mathrm{Tr}_s \left[\langle \, [H; \bar{N}_i^{\rho}] \, \rangle \right] \tag{2.18}$$

where $[H; \bar{N}_i^{\rho}]$ means the matrix with the commutator elements $[H; N_{i,\eta\eta'}^{\rho}]$ and the ρ-index shows where the current is calculated.

With this formulation the current and torque are now the components of the time derivative of the spin-occupation operator (J_i^ρ - from here on called the current).

$$\begin{aligned} J_{electric} &= -e\left\langle J_0^\alpha \right\rangle \\ \tau_x &= \frac{\hbar}{2}\left\langle J_1^{QD} \right\rangle \\ \tau_y &= \frac{\hbar}{2}\left\langle J_2^{QD} \right\rangle \\ \tau_z &= \frac{\hbar}{2}\left\langle J_3^{QD} \right\rangle \end{aligned} \tag{2.19}$$

The current in the leads

The zero-component (electric) of the spin occupation current in the leads is simple because the occupation operator commutes with all the parts of the Hamiltonian except the tunnelling part. The commutator with the tunnelling part and the spin-occupation matrix is

$$[H_T; N^\alpha_{i,\eta\eta'}] = \sum_{\substack{kn \\ \sigma\gamma}} \left(-\sigma_{i,\eta'\gamma} V_{k\alpha\gamma,n\sigma} a^\dagger_{k\alpha\eta} d_{n\sigma} + \sigma_{i,\eta'\gamma} V^*_{n\sigma,k\alpha\eta} d^\dagger_{n\sigma} a_{k\alpha\gamma} \right) \tag{2.20}$$

Here the commutator relation in equation (B.7) has been used.

The current through the quantum dot

The spin components of the spin occupation operator commute with fewer part of the Hamiltonian that the current component. The non-zero parts can for obvious reasons be named: The precession term, the tunnelling term and the interaction term

$$[H; N^{QD}_{i,\eta\eta'}] = [H_0; N^{QD}_{i,\eta\eta'}] + [H_T; N^{QD}_{i,\eta\eta'}] + [H_{int}; N^{QD}_{i,\eta\eta'}]$$

Precession term

The precession term is easily found

$$\begin{aligned} -2i\tau_i^{press} = Tr_s\left[H_0^{QD}; \bar{N}_i\right] &= Tr_s\Big[M_j\left[\sigma_j; \sigma_i\right]\Big] \\ &= -Tr_s\left[\epsilon_{ijk}\sigma_k M_j\right] = Tr_s\left[\left(\vec{\sigma}\times\vec{M}\right)_i\right] \end{aligned} \tag{2.21}$$

$\vec{M}$ has only a z-component. Hence all the factors in the cross product involving σ_z vanish because they are always multiplied with the x- or y-component of M. This leaves us with the σ_x and σ_y terms. These will also vanish because

the trace of these matrices are zero. The fact that this term vanishes should not be a big surprise. The kinetic and magnetic parts should not generate a torque by themselves.

Tunneling term

The tunneling term is found as in 2.20

$$[H_T; N^{QD}_{i,\eta\eta'}] = \sum_{\substack{n\alpha\sigma \\ \gamma}} \left(\sigma_{i,\eta'\gamma} V_{k\alpha\sigma,n\eta} a^\dagger_{k\alpha\sigma} d_{n\gamma} - \sigma_{i,\eta'\gamma} V^*_{n\gamma,k\alpha\sigma} d^\dagger_{n\eta} a_{k\alpha\sigma} \right) \tag{2.22}$$

The tunneling terms in the spin occupation current are the most important and we will continue with their determination later on.

Interaction term

This term depends on the type of interaction which is put on the dot. For the Coulomb interaction it can be easily show that this term vanishes because the interaction commutes with the spin operators. Other types of interactions could give a finite contribution but this discussion is left for future studies.

The current Green's function

The current depends on the expectation value of a combination of a lead and a dot operator - the tunneling terms. These expectation values can be expressed in forms of Green's functions which is discussed further in chapters 3 and 4. Two current Green's functions are defined as

$$\begin{aligned} G^<_{n\sigma',k\alpha\sigma}(t,t') &= i \left\langle a^\dagger_{k\alpha\sigma}(t') d_{n\sigma'}(t) \right\rangle \\ G^<_{k\alpha\sigma,n\sigma'}(t,t') &= i \left\langle d^\dagger_{n\sigma'}(t') a^\dagger_{k\alpha\sigma}(t) \right\rangle \end{aligned} \tag{2.23}$$

The $<$-index means that the Green's functions are of the lesser type due to their structure. The functions are connected by the identity

$$G^<_{k\alpha\sigma,n\sigma'}(t,t') = -\left(G^<_{n\sigma',k\alpha\sigma}(t,t') \right)^* = -G^{<*}_{k\alpha\sigma,n\sigma'}(t,t')$$

This means that the tunneling terms can be written as

$$\begin{aligned} i \left\langle [H_T; \bar{N}^\alpha_{i,\eta\eta'}] \right\rangle &= -\sum_{\substack{kn \\ \sigma\gamma}} \sigma_{i,\eta'\gamma} \left(V_{k\alpha\gamma,n\sigma} G^<_{n\sigma,k\alpha\eta}(t,t) + G^{<*}_{k\gamma\eta',n\sigma}(t,t) V^*_{n\sigma,k\alpha\eta} \right) \\ i \left\langle [H_T; \bar{N}^{QD}_i] \right\rangle &= \sum_{\substack{kn\alpha \\ \sigma\gamma}} \sigma_{i,\eta'\gamma} \left(G^<_{n\gamma,k\alpha\sigma}(t,t') V_{k\alpha\sigma,n\eta} + V^*_{n\gamma,k\alpha\sigma} G^{<*}_{k\alpha\sigma,n\eta}(t,t) \right) \end{aligned} \tag{2.24}$$

2.2.3 The preliminary trace formula

The expressions can be further simplified. This is most easily seen in matrix notation. Considering the leads, we have

$$i\left\langle [H_T;\bar{N}_i^\alpha]\right\rangle = -\sum_{kn}\left(\sigma_i\left(V_{k\alpha,n}G^<_{n,k\alpha}(t,t)+\left(V_{k\alpha,n}G^<_{n,k\alpha}(t,t)\right)^\dagger\right)\right)^T$$

The tunneling term has the form of a product of a sigma matrix and a sum of a matrix and its Hermitian conjugate. Recalling that we are interested in the trace of this matrix product we can first neglect the transpose operation - due to the transpose invariance of the trace operation. Next we can utilize the relation

$$\mathrm{Tr}_s[\sigma_i(\bar{M}+\bar{M}^\dagger)] = 2\,\mathbf{Re}\left\{\mathrm{Tr}_s\left[\sigma_i\bar{M}\right]\right\} \tag{2.25}$$

This enables us to write the expectation values in (2.19) in terms of a general tunneling current I^α

$$I_i^{\alpha,lead} = 2\mathbf{Re}\left\{\sum_{k,n}\mathrm{Tr}_s\left[\bar{\sigma}_0\bar{V}_{k\alpha n}\bar{G}^<_{n,k\alpha}(t,t)\right]\right\} \tag{2.26}$$

$$I_i^{\alpha} = 2\mathbf{Re}\left\{\sum_{k,n}\mathrm{Tr}_s\left[\bar{\sigma}_i\bar{G}^<_{n,k\alpha}(t,t)\bar{V}_{k\alpha n}\right]\right\} \tag{2.27}$$

The only difference between the two tunneling currents is the order of multiplication. In this thesis, we only consider the electric current in the leads. Therefore it is only the σ_0 which is used in the lead version of the current. The identity matrix commutes with all matrices hence we only need to consider the dot definition of the tunneling current. The electric current and the torques are now expressed as

$$J_e^\alpha = \frac{-e}{\hbar}I_0^\alpha \tag{2.28}$$

$$\tau_x = \frac{1}{2}\left(\sum_\alpha I_1^\alpha + \mathrm{Tr}_s\left\langle [H_{int}^{QD};N_1^{QD}]\right\rangle\right) \tag{2.29}$$

$$\tau_y = \frac{1}{2}\left(\sum_\alpha I_2^\alpha + \mathrm{Tr}_s\left\langle [H_{int}^{QD};N_2^{QD}]\right\rangle\right) \tag{2.30}$$

$$\tau_z = \frac{1}{2}\left(\sum_\alpha I_2^\alpha + \mathrm{Tr}_s\left\langle [H_{int};N_3^{QD}]\right\rangle\right) \tag{2.31}$$

The only unknown in the expression of I_i^α is the lesser Green's function defined in 2.23. This function can be determined in different ways depending on the model. We consider a model where the system is driven away from equilibrium by a time independent bias voltage applied to the contacts/leads. Therefore we have to use non-equilibrium theory to find this current Green's function.

CHAPTER 3

Non-equilibrium quantum field theory

The system considered in chapter 2 is not in equilibrium due to the finite bias voltage of the contacts ($\mu_L \neq \mu_R$). This means that we will have to use non-equilibrium quantum statistical mechanics to determine the lesser Green's function (2.23). This theory evolved from the works of Martin and Schwinger [22] and Schwinger [32] and was further developed by Kadanoff and Baym [16], and by Keldysh [17]. The formulation used in this thesis is due to Keldysh and based on the form presented by Langreth [20]. Furthermore this presentation is inspired by the presentations in Rammer and Smith[31], Haug and Jauho [10] and Ferry and Goodnick [7]. The presentation is focused on the aspects of the theory that we will need.

It has been argued that the method is only valid when the entropy production is relatively small and the system remains close to equilibrium (see [7] for discussion). However the method has successfully been used in strongly far-from-equilibrium systems and is the method used in Jauho, Wingreen and Meir [12] which forms the basis for various treatments on resonant tunneling systems ([24],[33]).

In section 3.1 the non-equilibrium theory and the perturbation expansion of the contour ordered Green's function are introduced and in section 3.2 derives the rules of analytic continuation and the Dyson equations are derived.

3.1 Contour ordered Green's functions

The non-equilibrium problem is formulated as a system evolving under a Hamiltonian having the form

$$\mathcal{H} = H + H'(t) = H_0 + H_i + H'(t) \tag{3.1}$$

The time independent part (H) is split into a quadratic part (H_0) and a part containing the many-body interactions (H_i) in the system. The non-equilibrium part ($H'(t)$) is assumed to vanish for times $t < t_0$. This non-equilibrium part is the difference between the chemical potentials of the leads in the model. It was shown in section 2.2 how the physical observables (the elements of the general current) are expressed in terms of the lesser Green's functions. The expectation value of an observable is found in non-equilibrium statistical mechanics at times $t > t_0$ using the formula

$$\langle O_{\mathcal{H}}(t)\rangle = \mathbf{Tr}\left[\rho(H)O_{\mathcal{H}}(t)\right] \tag{3.2}$$

where $\rho(H) = \left(\mathbf{Tr}\exp\left(-\beta H\right)\right)^{-1}\exp\left(-\beta H\right)$ is the equilibrium density matrix and O is the observable. Here the brackets $\langle\cdots\rangle$ mean the expectation value. The subscript $\mathcal{H}$ means that the time dependence is governed by the full Hamiltonian. The problem lies in determining the complicated time dependence of $O_{\mathcal{H}}$. The trick which is analogously to the equilibrium method is to transform the time dependence to O_{H_0} and then use Wick's theorem which is then applicable because H_0 is quadratic in the field operators.

The manipulations needed to determine the Green's functions are most easily and compactly done by defining the contour (path) ordered Green's function

$$G(1,1') = -i\left\langle T_C\Psi_{\mathcal{H}}(1)\Psi^{\dagger}_{\mathcal{H}}(1')\right\rangle \tag{3.3}$$

where C is a complex contour along the real axis (or near it) that begins and ends at t_0 and passes through t and t' once - see figure 3.1. The notation 1 implies the set (τ,ν) where ν includes the variables needed to define the operators and τ is the complex time. The contour ordering operator T_C orders the operators accordingly to their positions on the contour. Here the brackets denotes an average over the accessible phase space. The transformations needed to put the Green's function into the interaction picture with respect to H_0 are fully described in Rammer and Smith [31]. The Green's function then acquires the following form

$$G(1,1') = -i\frac{\langle T_C S_{C_m} S_C \Psi_{H_0}(1)\Psi^{\dagger}_{H_0}(1')\rangle_0}{\langle T_C S_{C_m} S_C\rangle_0} \tag{3.4}$$

where the transformation operators are defined as

$$S_{C_m} = \exp\left(-i\int_{C_i} d\tau H^i_{H_0}(\tau)\right) \tag{3.5}$$

$$S_C = \exp\left(-i\int_{C} d\tau H'_{H_0}(\tau)\right) \tag{3.6}$$

The contours can be seen in figure 3.1. The abstract structure of the Green's function is now seen to be identical to that of the equilibrium Green's functions e.g. the finite temperature Matsubara Green's functions [4]. The perturbation expansion (Feynman diagrams) of the contour ordered Green's

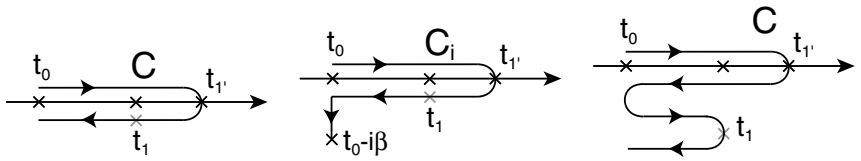

Figure 3.1: The different contours discussed in this section. The left is the one used in the definition of the contour ordered Green's function and the center is used in the transformation which puts the operators into the interaction picture with respect to H_0. The right is the contour used in the determination of the rules of analytical continuity.

functions can therefore be mapped onto the equilibrium perturbation expansion (Feynman diagrams).

3.2 Analytic continuation

Being more comfortable with the contour ordered Green's functions we will continue with the method of analytic continuation. The method is due to Langreth [20] and is a set of rules for calculating objects which are products of contour ordered objects. Considering an object that is a product of two other path ordered functions.

$$D(t,t') = \int_C d\tau A(t,\tau)B(\tau,t') \tag{3.7}$$

D is independent of the choice of contours with the same endpoints (t,t') and direction. Using a closed contour starting at t_0 going to t, back to t_0 through t' before ending at t_0 it can be easily shown that in the limit $t_0 = -\infty$ [1] the contour objects can be calculated on the real axis following the rules

$$D^r(t,t') = \int_{-\infty}^{\infty} dt_1 A^r(t,t_1)B^r(t_1,t') \tag{3.8}$$

$$D^<(t,t') = \int_{-\infty}^{\infty} dt_1 A^r(t,t_1)B^<(t_1,t') + A^<(t,t_1)B^a(t_1,t') \tag{3.9}$$

where the retarded and advanced Green's functions have been introduced

$$G^r(1,1') = -i\theta(\tau-\tau')\left\langle\left\{\Psi(1);\Psi^\dagger(1')\right\}\right\rangle \tag{3.10}$$

$$G^a(1,1') = +i\theta(\tau'-\tau)\left\langle\left\{\Psi(1);\Psi^\dagger(1')\right\}\right\rangle \tag{3.11}$$

[1] The contribution from the part of the contour from t_0 to $t_0 - i\beta$ vanishes in this limit. This is true because we do not consider the initial correlations of the system. Se [31] for a more elaborate discussion.

where $\{\ ;\ \}$ is the anticommutator. The advanced function is the complex conjugate of the retarded one. These rules can be generalized to products of more functions but that will not be needed here.

The non-equilibrium Dyson equation for the contour ordered function is in matrix notation

$$G = G_0 + G_0 \Sigma G \tag{3.12}$$

Using the rules of analytic continuation we get

$$G^{r(a)} = G_0^{r(a)} + G_0^{r(a)} \Sigma^{r(a)} G^{r(a)} \tag{3.13}$$

$$G^{<} = G^r \Sigma^{<} G^a \tag{3.14}$$

The retarded(advanced) follow easily. The lesser Dyson equation also known as the Keldysh equation is more tedious to derive. We iterate the Dyson equation with the lesser continuation rule (3.9). In the iterative limit we find

$$G^{<} = (1 + G^r \Sigma^r) G_0^{<} (1 + \Sigma^a G^a) + G^r \Sigma^{<} G^a \tag{3.15}$$

The first term is zero. This is shown in two steps. First the retarded Dyson equation gives $(1 + G^r \Sigma^r) G_0^{<} = G^r (G_0^r)^{-1} G_0^{<}$. Secondly the equation of motion for the lesser bare Green's function gives $(G_0^r)^{-1} G_0^{<} = 0$.

This concludes the review of the topics of non-equilibrium quantum field theory we will need in the following chapter.

CHAPTER 4

General trace formula (GTF)

This chapter contains the derivation of the general trace formula for both the electric current and the spin torque. The formula takes its name from its form. The currents are expressed as a trace over spin and dot quantum numbers of a matrix consisting of level width functions and Green's functions.

In the first section the current Green's function (2.23) will be decomposed into a product of a lead and a dot Green's function. Then the rules of analytic continuation (section 3.2) will be used on this product to give an expression for the current. Due to the steady state assumption the time integral can be performed and the final trace formula found. Different symmetric forms and a scaling of the general trace formula are discussed. In the last section a proportionate coupling is discussed because of the possibility of eliminating the most troublesome term in the current trace equation.

4.1 First trace formula

As discussed in the previous section the current Green's function is defined on a path in the complex time plane. This is symbolized by the use of τ as the time variable. The current Green's function is defined as (2.23)

$$G_{m\mu,k\alpha\eta}(\tau,\tau') = i\langle a^{\dagger}_{k\alpha\eta}(\tau')d_{m\mu}(\tau)\rangle$$

where τ and τ' lie on the contour. The noninteracting leads in the model insure that the Green's function can be decomposed into a product of a lead- and a dot Green's function. This decomposition is here done with the use of Feynman diagrams.

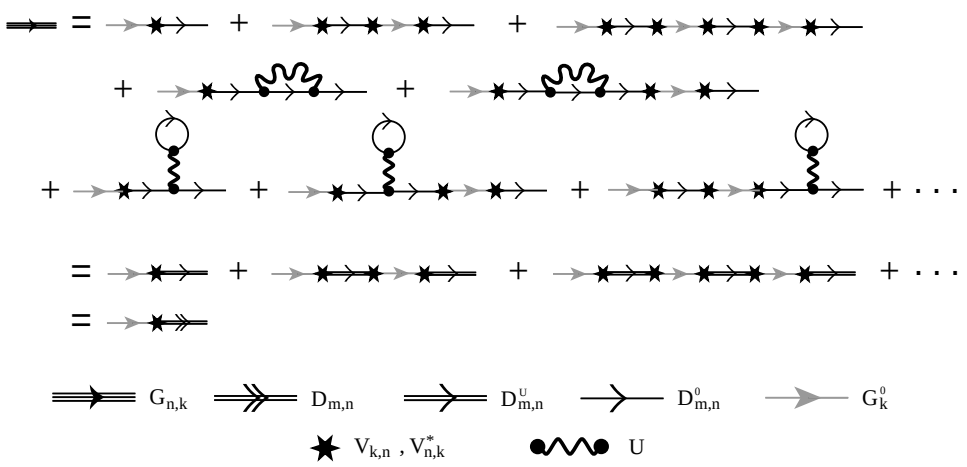

Figure 4.1: Decomposition of the current Green's function into the free lead and full dot Green's functions. The current Green's function is expanded in the tunneling and dot-interactions. As a model for the dot-interactions is used the Coulomb model discussed in chapter 6. The Green's functions used in the diagram are defined in the text except for the interacting dot-Green's function (D^U) which is only used as an intermediate function.

In the previous chapter it was seen that the Feynman diagrams of a contour ordered object maps into the Feynman diagrams of the same object in equilibrium. The current Green's function is expanded in the tunneling and dot-interactions.

The result of the expansion is

$$\bar{G}_{m,k\alpha}(\tau,\tau') = \sum_n \int_C d\tau_2 \bar{D}_{m,n}(\tau,\tau_2)\bar{V}^\dagger_{n,k\alpha}\bar{G}^0_{k\alpha}(\tau_2,\tau') \tag{4.1}$$

where the full dot-Green's function is defined as

$$D_{m\mu,n\nu}(\tau,\tau') = (-i)\langle T_C \bar{S}\tilde{d}_{m\mu}(\tau)\tilde{d}^\dagger_{n\nu}(\tau')\rangle \tag{4.2}$$

and the free lead Green's function has the form

$$G^0_{k\alpha\eta} = (-i)\langle T_C \tilde{a}^\dagger_{k\alpha\eta}(\tau')\tilde{a}_{q\beta\eta'}(\tau_2)\rangle \delta(k-q)\delta_{\alpha\beta}\delta_{\eta\eta'} \tag{4.3}$$

The current Green's function has been decomposed into a product of two other Green's functions. The analytic pieces of this product are found using the rules of analytic continuation. Combining (4.1) and (3.9) it is found that

$$\begin{aligned}\bar{G}^<_{m,k\alpha}(t,t') = \sum_n \int dt_2 \Big(& \bar{D}^<_{m,n}(t,t_2)\bar{V}^\dagger_{n,k\alpha}\bar{G}^{0,a}_{k\alpha}(t_2,t') \\ & + \bar{D}^r_{m,n}(t,t_2)\bar{V}^\dagger_{n,k\alpha}\bar{G}^{0,<}_{k\alpha}(t_2,t')\Big)\end{aligned} \tag{4.4}$$

When the expression for the current Green's function is used, the formulas for the tunneling current become

$$I_i^\alpha(t) = 2\mathbf{Re}\Big\{ \sum_{nm,k} \int dt_2 \mathrm{Tr}\Big[\bar{\sigma}_i \Big(\bar{D}^<_{n,m}(t,t_2)\bar{V}^\dagger_{m,k\alpha}\bar{G}^{0,a}_{k\alpha}(t_2,t) + \bar{D}^r_{n,m}(t,t_2)\bar{V}^\dagger_{m,k\alpha}\bar{G}^{0,<}_{k\alpha}(t_2,t)\Big)\bar{V}_{k\alpha,n}\Big]\Big\} \tag{4.5}$$

In the following calculation the expression for the current in the leads has been used. It is straight-forward to apply the same calculations to the quantum dot current.

The leads are non-interacting and their Green's functions are well known ([4])

$$\begin{aligned} G^{0,a}_{k\alpha\eta}(t,t') =& i\theta(t'-t)e^{-i\epsilon_{k\alpha\eta}(t-t')} \\ G^{0,<}_{k\alpha\eta}(t,t') =& i f_\alpha(\epsilon_{k\alpha\eta})e^{-i\epsilon_{k\alpha\eta}(t-t')} \end{aligned}$$

where $f_\alpha(\epsilon_{k\alpha\eta})$ is the Fermi function and $\epsilon_{k\alpha\eta}$ is the entry in the lead energy matrix $\bar{\mathcal{E}}_{k\alpha}$ defined in (2.5). Inserting these functions into the two terms of the tunneling current expression we have

$$i \sum_{\substack{kmn \\ \eta\mu\mu'\nu}} \sigma_{i,\mu\mu'} D^<_{m\mu',n\nu}(t,t_2) V^*_{n\nu,k\alpha\eta}\theta(t-t_2)e^{-i\epsilon_{k\alpha\eta}(t_2-t)}V_{k\alpha\eta,m\mu} \tag{4.6}$$

$$i \sum_{\substack{kmn \\ \eta\mu\mu'\nu}} \sigma_{i,\mu\mu'} D^R_{m\mu',n\nu}(t,t_2) V^*_{n\nu,k\alpha\eta} f_\alpha(\epsilon_{k\alpha\eta})e^{-\epsilon_{k\alpha\eta}(t_2-t)}V_{k\alpha\eta,m\mu} \tag{4.7}$$

Consider the second term, it can be evaluated as (the first term follows the exact same steps)

$$\begin{aligned} & i \sum_{\substack{kmn \\ \eta\mu\mu'\nu}} D^R_{m\mu',n\nu}(t,t_2) V^*_{n\nu,k\alpha\eta} f_\alpha(\epsilon_{k\alpha\eta})e^{-\epsilon_{k\alpha\eta}(t_2-t)}V_{k\alpha\eta,m\mu}\sigma_{i,\mu\mu'} \\ & \quad = i \sum_{\substack{nm \\ \mu\mu'\nu}} \int \frac{d\epsilon}{2\pi} f_\alpha(\epsilon)e^{-\epsilon(t_2-t)}\sigma_{i,\nu\nu'}D^R_{m\mu',n\nu}(t,t_2)\Gamma^\alpha_{n\nu,m\mu}(\epsilon) \end{aligned} \tag{4.8}$$

where the level width function $\bar{\Gamma}^\alpha_{m\mu,n\nu}(\epsilon)$ has been introduced. It will be shown in chapter 5 that the level width function is the imaginary part of the tunneling self-energy. The k-sum can be performed and it is seen that Γ only depends on the coupling amplitudes and the density of states in the

respective contact. Γ is sometimes refereed to the elastic coupling parameter [37].

$$\begin{aligned}\Gamma^{\alpha}_{m\mu,n\nu}(\epsilon) =& 2\pi \sum_{k\gamma} \delta(\epsilon - \epsilon_{k\alpha\gamma}) V^{*}_{m\mu,k\alpha\gamma} V_{k\alpha\gamma,n\nu} \\ =& 2\pi \sum_{\gamma} \rho_{\alpha\gamma}(\epsilon) V^{*}_{m\mu,\alpha\gamma}(\epsilon) V_{\alpha\gamma,n\nu}(\epsilon)\end{aligned} \tag{4.9}$$

Here $V_{\alpha\gamma,n\nu}(\epsilon)$ means the coupling amplitude with the k for which $\epsilon_k = \epsilon$. Gathering the new expressions for the terms in the tunneling current we have

$$\begin{aligned}I^{\alpha}_{i}(t) = 2\mathbf{Im}\Bigg\{ \int \frac{d\epsilon}{2\pi} \int_{-\infty}^{t} dt_2 e^{-i\epsilon(t_2 - t)} \\ \mathrm{Tr}_{n,s}\left[\bar{\mathbf{\Gamma}}^{i,\alpha}(\epsilon) \left(\bar{\mathbf{D}}^{<}(t,t_2) + f_{\alpha}(\epsilon) \bar{\mathbf{D}}^{R}(t,t_2) \right) \right] \Bigg\}\end{aligned} \tag{4.10}$$

where the boldface notation imply matrices in the middle region indices, $\mathrm{Tr}_{n,s}$ indicates a trace in these indices and spin. The limits on the time integral originate from the θ-function in (4.6) and also apply to the other term (4.7) because D^r is zero for times greater than t.

4.2 The General Trace Formula

The model is a steady state model and therefore the quantities are time independent[1]. This means that the time-integral in (4.10) can be performed. The two terms are integrated separately.

Lesser term

$$\begin{aligned}&\mathbf{Im}\Bigg\{ \int \frac{d\epsilon}{2\pi} \int_{-\infty}^{t} dt_2 e^{-i(\epsilon + ic)(t_2 - t)} \mathrm{Tr}_{n,s}\left[\bar{\mathbf{\Gamma}}^{i,\alpha}(\epsilon) \int \frac{d\omega}{2\pi} e^{-i\omega(t - t_2)} \bar{\mathbf{D}}^{<}(\omega) \right] \Bigg\} \\ &\quad = \mathbf{Re}\Bigg\{ \int \frac{d\epsilon}{2\pi} \int \frac{d\omega}{2\pi} \mathrm{Tr}_{n,s}\left[\frac{\bar{\mathbf{\Gamma}}^{\alpha}(\epsilon) \sigma_i \bar{\mathbf{D}}^{<}(\omega)}{\epsilon - \omega + ic} \right] \Bigg\} \\ &\quad = \frac{1}{2} \int \frac{d\epsilon}{2\pi} \int \frac{d\omega}{2\pi} \mathrm{Tr}_{n,s}\left[\frac{\bar{\mathbf{\Gamma}}^{\alpha}(\epsilon) \sigma_i \bar{\mathbf{D}}^{<}(\omega)}{\epsilon - \omega + ic} - \frac{\left(\bar{\mathbf{\Gamma}}^{\alpha}(\epsilon)\right)^{t} \sigma_i^{t} \left(\bar{\mathbf{D}}^{<}(\omega)\right)^{t}}{\epsilon - \omega - ic} \right]\end{aligned} \tag{4.11}$$

Identities involving the complex conjugate of the level width function, the sigma matrices and dot-Green's functions (B.3) have been used in the last equality.

[1] The theory could be expanded to include time dependent phenomena by following the method used in [12].

The ϵ-integral can be evaluated as

$$\begin{aligned}\frac{1}{2}\int\frac{d\omega}{2\pi}P\int\frac{d\epsilon}{2\pi}\mathrm{Tr}_{n,s}\left[\frac{\bar{\mathbf{\Gamma}}^{\alpha}(\epsilon)\sigma_i\bar{\mathbf{D}}^{<}(\omega)-\bar{\mathbf{D}}^{<}(\omega)\sigma_i\bar{\mathbf{\Gamma}}^{\alpha}(\epsilon)}{\epsilon-\omega}\right]\\ +\frac{-i}{4}\int\frac{d\omega}{2\pi}\mathrm{Tr}_{n,s}\left[\bar{\mathbf{\Gamma}}^{\alpha}(\omega)\left(\sigma_i\bar{\mathbf{D}}^{<}(\omega)+\bar{\mathbf{D}}^{<}(\omega)\sigma_i\right)\right]\end{aligned} \tag{4.12}$$

Where $P\int$ is the principal value integral. The transposed invariance of a trace has been used in the principal value integral. If we consider the electric current the σ_i can be removed and the cyclic properties can be used to eliminate the principal value integral. Furthermore the second term combines into a single factor $\bar{\mathbf{\Gamma}}^{\alpha}(\omega)\bar{\mathbf{D}}^{<}(\omega)$. For the spin torque the principal value integral will have to be determined.

Retarded term

The retarded is much easier. The dot-Green's function is zero for all times greater than t, so the upper limit of the integral can be extended to infinity. Then it is the Fourier transformed dot-Green's function.

$$\begin{aligned}\mathrm{Im}\left\{\int\frac{d\epsilon}{2\pi}f_{\alpha}(\epsilon)\mathrm{Tr}_{n,s}\left[\bar{\mathbf{\Gamma}}^{\alpha}(\epsilon)\sigma_i\int\frac{d\omega}{2\pi}\bar{\mathbf{D}}^{R}(\epsilon)\right]\right\}\\ =\frac{-i}{2}\int\frac{d\epsilon}{2\pi}f_{\alpha}(\epsilon)\mathrm{Tr}_{n,s}\left[\bar{\mathbf{\Gamma}}^{\alpha}(\epsilon)\left(\sigma_i\bar{\mathbf{D}}^{r}(\epsilon)-\bar{\mathbf{D}}^{a}(\epsilon)\sigma_i\right)\right]\end{aligned} \tag{4.13}$$

4.2.1 Different formulations of GTF

Gathering the results from the previous sections we can formulate the final version of the general trace formula. In the future discussions and calculations we have to use different versions of the GTF because different tricks can be used. Therefore the formula will be formulated in in different versions. Due to clarity the electrical current and the spin torque will be presented separately.

Electrical current

The formula for the electric current is the most simple and the result is the same as others have found before [33] [35] [38]. The difference between this formulation and that of others is the separation of the spin variables and the general nature of the level width functions. This allows for a detailed analysis of the electric currants dependence on spin related phenomena. Combining the results in (4.13), (4.12) and (2.28) and remembering that the principal value integral vanishes in the case of the electric current, we obtain

GTF electrical current

$$J_e^\alpha = \frac{ie}{\hbar}\int \frac{d\omega}{2\pi}\mathrm{Tr}_{n,s}\left[\bar{\mathbf{\Gamma}}^\alpha(\omega)\left(\bar{\mathbf{D}}^<(\omega) + f_\alpha(\omega)\left(\bar{\mathbf{D}}^r(\epsilon) - \bar{\mathbf{D}}^a(\epsilon)\right)\right)\right] \tag{4.14}$$

The form of this equation can be understood in terms of local distribution functions. The lesser term is proportionate to the occupation of the dot and can therefore be related to tunneling-out from the dot. The second term is proportional to the occupation of the lead and can be related to the tunneling-in [12].

Using the Keldysh equation (3.14) and the relation $D^r - D^a = D^r \Sigma D^a$ where $\Sigma = \Sigma^r - \Sigma^a$ the trace formula become more compact

GTF electrical current with Keldysh equation

$$J_e^\alpha = \frac{ie}{\hbar}\int \frac{d\omega}{2\pi}\mathrm{Tr}_{n,s}\left[\bar{\mathbf{\Gamma}}^\alpha(\omega)\bar{\mathbf{D}}^r(\epsilon)\left(\bar{\mathbf{\Sigma}}^<(\omega) + f_\alpha(\omega)\bar{\mathbf{\Sigma}}(\omega)\right)\bar{\mathbf{D}}^a(\epsilon)\right] \tag{4.15}$$

In some cases, it can be useful to apply the symmetric formula. The symmetric current is $J_e = \frac{1}{2}\left(J_e^L - J_e^R\right)$ giving

Symmetric GTF electrical current

$$\begin{aligned} J_e^\alpha = \frac{ie}{\hbar}\int \frac{d\omega}{2\pi}\mathrm{Tr}_{n,s}\Big[&\left(\bar{\mathbf{\Gamma}}^L(\omega) - \bar{\mathbf{\Gamma}}^R(\omega)\right)\bar{\mathbf{D}}^<(\omega) + \\ &\left(f_L\bar{\mathbf{\Gamma}}^L(\omega) - f_R\bar{\mathbf{\Gamma}}^R(\omega)\right)\left(\bar{\mathbf{D}}^r(\epsilon) - \bar{\mathbf{D}}^a(\epsilon)\right)\Big] \end{aligned} \tag{4.16}$$

Spin torque

The formulas for the spin torque are more cumbersome. We cannot do anything about the principal integral in (4.12) at the moment. It will be discussed again in section 7.1.1. Combining the results in (4.13), (4.12) and (2.29-2.29)

Spin torque

$$\tau_i = -\frac{i}{2}\int \frac{d\omega}{2\pi}\mathrm{Tr}_{n,s}\Big[\bar{\mathbf{T}}^{\alpha}_{principal} + \frac{1}{2}\Big(\bar{\mathbf{\Gamma}}(\omega)\sigma_i + \sigma_i\bar{\mathbf{\Gamma}}(\omega)\Big)\bar{\mathbf{D}}^{<}(\omega) + \Big(f_\alpha(\omega)\bar{\mathbf{\Gamma}}^{L} + f_\alpha(\omega)\bar{\mathbf{\Gamma}}^{L}\Big)(\omega)\Big(\sigma_i\bar{\mathbf{D}}^{r}(\omega) - \bar{\mathbf{D}}^{a}(\omega)\sigma_i\Big)\Big] \quad (4.17)$$

$$\bar{\mathbf{T}}^{\alpha}_{principal} = 2iP\int \frac{d\epsilon}{2\pi}\frac{\bar{\mathbf{\Gamma}}^{\alpha}(\epsilon)\sigma_i\bar{\mathbf{D}}^{<}(\omega) - \bar{\mathbf{D}}^{<}(\omega)\sigma_i\bar{\mathbf{\Gamma}}^{\alpha}(\epsilon)}{\epsilon - \omega}$$

where $\bar{\mathbf{\Gamma}}(\omega)$ is the sum of the left and right level width functions.

4.3 Scaling of the GTF

When comparing with experiments or other theoretical works it is often easier to compare dimensionless quantities. This also removes some of the sample dependence from experimental results. Therefore the energy of the integral is scaled in units of the left up-up tunneling level width. This has the consequence that the gamma's change their form from

$$\bar{\Gamma}^{\alpha}_{m,n}(\epsilon) = U^{\dagger}_{\alpha}\mathcal{T}^{\alpha}U_{\alpha} \quad (4.18)$$

$$\mathcal{T}^{\alpha}_{m,n} = 2\pi\begin{bmatrix} |t_{\epsilon,\uparrow}|^2\rho_{\alpha\uparrow}(\epsilon) & 0 \\ 0 & |t_{\epsilon,\downarrow}|^2\rho_{\alpha\downarrow}(\epsilon)\end{bmatrix} \quad (4.19)$$

to the scaled form

$$\bar{\Gamma}^{L}_{m,n}(\epsilon) = U^{\dagger}_{L}\mathcal{T}^{L}U_{L} \quad (4.20)$$

$$\bar{\Gamma}^{R}_{m,n}(\epsilon) = \lambda U^{\dagger}_{R}\mathcal{T}^{R}U_{R} \quad (4.21)$$

$$\mathcal{T}^{\alpha}_{m,n} = \begin{bmatrix} 1 & 0 \\ 0 & \gamma_\alpha\end{bmatrix} \quad (4.22)$$

where γ_α is the fraction of the up to the down matrix element in (4.19) and will be referred to as the polarization of the lead. λ is the fraction of the right up element to the left up element and is referred to as the asymmetry of the leads. This scaling means that the energy scale is in units of the left up-up tunneling level.

The tunneling amplitudes have been assumed dependent on k and n. In the following chapters this will not be necessary because we will not consider processes where this dependence is important[2].

[2]If the calculations included the spin-orbit coupling the diagonal spin-basis on the dot would depend on n and therefore also the tunneling amplitudes.

4.4 Proportionate coupling

The largest problem in the trace formula (4.17) is the determination of the lesser Green's function. In the non-interacting case it can be found explicitly but when the Coulomb interaction is turned on, we have to rely on approximative and numerical methods (sec. 6.3.3). In [12] it is demonstrated that under certain circumstances the lesser term can be eliminated. This happens if it is assumed that the linewidth functions are proportional and the electric current is written as a combination of the left- and right current.

$$\bar{\mathbf{\Gamma}}^L(\omega) = \lambda \bar{\mathbf{\Gamma}}^R(\omega) \tag{4.23}$$

$$J_e = x J_e^L - (1-x)\, J_e^R \tag{4.24}$$

Using equation (4.14) and (4.23) the lesser term disappears if $\lambda = \frac{1-x}{x}$. Unfortunately, it is only under certain angle conditions that the level width functions can be proportionate for magnetic contacts. Assuming that the tunneling matrices $\bar{\mathcal{T}} = \bar{T}^\dagger \bar{\rho} \bar{T}$ are diagonal the following relation is found.

$$\bar{\mathcal{T}}_L = \lambda \bar{S}^\dagger \bar{\mathcal{T}}_R(\epsilon) \bar{S} \tag{4.25}$$

where $\bar{S} = \bar{U}_{Rn} \bar{U}^\dagger_{Lm}$. This relation shows that a proportionate coupling is possible if the matrix product on the right side of the equality is diagonal. This is generally not true but can occur for special configurations. $\bar{S}$ is a rotation matrix and has the structure

$$\bar{S} = \begin{bmatrix} D & A \\ -A^* & D^* \end{bmatrix} \tag{4.26}$$

where A and D are dependent on the angles of rotation. The matrix product from (4.25) then becomes

$$\bar{S}^\dagger(\epsilon) \bar{\mathcal{T}}_R(\epsilon) \bar{S}(\epsilon) = \begin{bmatrix} D^2\mathcal{T}_\uparrow + A^2\mathcal{T}_\downarrow & D^*A(\mathcal{T}_\uparrow - \mathcal{T}_\downarrow) \\ DA^*(\mathcal{T}_\uparrow - \mathcal{T}_\downarrow) & A^2\mathcal{T}_\uparrow + D^2\mathcal{T}_\downarrow \end{bmatrix} \tag{4.27}$$

This matrix is diagonal if one of three conditions are fulfilled:

1. $\mathcal{T}_\uparrow - \mathcal{T}_\downarrow = 0$ - this means that $t_\uparrow^2 \rho_\uparrow = t_\downarrow^2 \rho_\downarrow$ hence a normal metal. This condition is independent on the angles.
2. $A = 0$ this condition is dependent on the angles of rotations. The dependence on the rotations is found in the next section.
3. $D = 0$ this condition is also dependent on the rotation and the dependence is found in the next section. This condition implies that the left up tunneling should be equal to the right down tunneling and vice versa.

Angular dependence

The angular dependence of the second and third conditions are found in the following.

$A = 0$

This condition imply the following connection between the angles

$$\sin\left(\frac{\theta}{2}\right)\cos\left(\frac{\psi}{2}\right) = e^{i(\zeta-\phi)}\sin\left(\frac{\psi}{2}\right)\cos\left(\frac{\theta}{2}\right) \tag{4.28}$$

This condition is trivially fulfilled in the case when the two leads have parallel magnetizations. The exponential on the right hand side must be real. This imply that $\zeta - \phi = 0$ or $\zeta - \phi = \pi$. In the first case where the two azimuthal angles are identical the two polar angels also need to be identical. This means that a proportionate coupling can be achieved if the magnetization of the leads are parallel with an arbitrary angle to the quantum dot magnetization. In the other case where the difference of the azimuthal angles is π the polar angles have to fulfill the relation $\theta + \psi = 0$. The polar angles are only defined in the interval $[0; \pi]$ hence the only configuration possible is the trivial parallel ($\theta = \psi = 0$) but with a phase difference of π.

$D = 0$

The relation the angles must fulfill to make this condition true is

$$\cos\left(\frac{\theta}{2}\right)\cos\left(\frac{\psi}{2}\right) + e^{i(\zeta-\phi)}\sin\left(\frac{\psi}{2}\right)\sin\left(\frac{\theta}{2}\right) = 0 \tag{4.29}$$

The same conditions apply to the phase angles as in the previous case. When the azimuthal angles are identical, it is found that $\theta = \psi + \pi$ – an anti-parallel configuration of the leads. In the other case where the azimuthal angles differ with π the polar angles have to fulfill the relation $\theta = \pi - \psi$. This configuration is where the left and right magnetizations are in an anti-parallel configuration with an arbitrary angle to the dot magnetization. The $D = 0$ condition therefore is fulfilled for an anti-parallel configuration. But the right tunneling matrix is already anti-parallel of the left matrix. Hence The configuration of the system is with parallel contact magnetizations.

4.5 GTF summary

This concludes the chapters concerning the general theory of the model. The electric current and spin torque have been determined and different expressions are presented in (4.14) to (4.17). The formulas have been expressed

in terms of dimensionless parameters (section 4.3) and finally it has been shown that in the parallel configuration of the leads the formulas simplify significantly.

CHAPTER 5

Non-interacting quantum dot

In this chapter the non interacting model is presented. This model is rather simple, but will give insight into the resonance phenomena. It has a close connection to the Coulomb model presented in the next chapter because it can be seen as the limit where the coupling is larger that the Coulomb interaction. This is discussed at length in chapter 7.

The model is solved exactly and the dot-Green's functions and self-energies are inserted into the general trace formulas for the electric current and the spin torques.

5.1 The non-interacting quantum dot Green's function

The non-interacting quantum dot Hamiltonian only has the diagonal part

$$H_{QD} = \sum_n \vec{d}_n^\dagger \cdot \bar{\mathcal{E}}_n \vec{d}_n \tag{5.1}$$

This means that the Green's functions can be found exactly. This is done using the equation of motion method. The retarded dot-Green's function is defined in (4.2) as

$$D^r_{m\mu,n\nu}(t-t') = -i\theta(t-t') \left\langle \left\{ d_{m\mu}(t); d^\dagger_{n\nu}(t') \right\} \right\rangle$$

The time derivative of the function is

$$i\partial_t D^r_{m\mu,n\nu}(t-t') = \delta(t-t')\delta_{mn}\delta_{\mu\nu} + (-i)\theta(t-t')\left\langle\left\{-[H;d_{m\mu}](t);d^\dagger_{n\nu}(t')\right\}\right\rangle \tag{5.2}$$

The commutator $[H;d_{m\mu}]$ is non-zero for the tunneling and the quantum dot parts of the Hamiltonian. These parts give

$$[H_0^{QD};d_{m\mu}] = \sum_{n\nu}\epsilon_{n\nu}[d^\dagger_{n\nu}d_{n\nu};d_{m\mu}] = -\epsilon_{m\mu}d_{m\mu} \tag{5.3}$$

$$[H_T;d_{m\mu}] = \sum_{\substack{nk\alpha\\ \sigma\sigma'}} V^*_{n\sigma,k\alpha\sigma'}[d^\dagger_{n\sigma}a_{a\alpha\sigma'};d_{m\mu}] = -\sum_{k\alpha\sigma'} V^*_{m\mu,k\alpha\sigma'}a_{a\alpha\sigma'} \tag{5.4}$$

This gives the equation of motion in frequency space

$$(\omega-\epsilon_{m\mu})D^r_{m\mu,n\nu}(\omega) = \delta_{mn}\delta_{\mu\nu} + \sum_{k\alpha\sigma} V^*_{m\mu,k\alpha\sigma}(\omega)F^r_{k\alpha\sigma,n\nu}(\omega) \tag{5.5}$$

where a new kind of Green's function is defined

$$F^r_{k\alpha\sigma,n\nu}(t-t') = -i\theta(t-t')\left\langle\left\{a_{k\alpha\sigma}(t);d^\dagger_{n\nu}(t')\right\}\right\rangle \tag{5.6}$$

This new Green's function is the propagator of an electron starting in the quantum dot at time t' and ending in the α-lead at time t. This tunneling Green' function is calculated the same way as the quantum dot function. In this calculation it is the lead and tunneling part of the Hamiltonian which give the non-zero contributions:

$$[H_0^{lead};a_{k\alpha\sigma}] = \sum_{q\beta\sigma'}\epsilon_{q\beta\sigma'}[a^\dagger_{q\beta\sigma'}a_{q\beta\sigma'};a_{k\alpha\sigma}] = -\epsilon_{k\alpha\sigma}a_{k\alpha\sigma} \tag{5.7}$$

$$[H_T;a_{k\alpha\sigma}] = \sum_{\substack{nq\beta\\ \eta\eta'}} V_{q\beta\eta,n\eta'}[a^\dagger_{q\beta\eta}d_{n\eta'};a_{k\alpha\sigma}b] = -\sum_{n\eta'} V_{k\alpha\sigma,n\eta'}d_{n\eta'} \tag{5.8}$$

This gives an EOM-equation for the tunneling Green's function

$$(\omega-\epsilon_{k\alpha\sigma})F^r_{k\alpha\sigma,n\nu}(\omega) = \sum_{m\mu} V_{k\alpha\sigma,m\mu}(\omega)D^r_{m\mu,n\nu}(\omega) \tag{5.9}$$

The free particle lead Green's function has the well known form [4]

$$G^{0,r}_{k\alpha\sigma}(\omega) = (\omega-\epsilon_{k\alpha\sigma})^{-1} \tag{5.10}$$

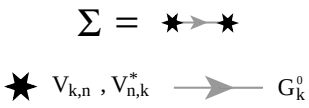

Figure 5.1: The Feynman diagram for the tunneling self-energy. The diagram consists of two vertices connected by a lead electron propagator.

Combining equation (5.5) and (5.9) we find an expression for the quantum dot Green's function

$$\bar{\mathbf{D}}^{\mathbf{r}}_{\Sigma}(\omega) = \left(\bar{\mathbf{E}}(\omega) - \bar{\mathbf{\Sigma}}^{r}_{0}(\omega)\right)^{-1} \tag{5.11}$$

where the retarded self-energy is defined as

$$\Sigma^{r}_{0,m\mu,l\eta}(\omega) = \sum_{k\alpha\sigma} V^{*}_{m\mu,k\alpha\sigma} G^{0,r}_{k\alpha\sigma}(\omega) V_{k\alpha\sigma,l\eta} \tag{5.12}$$

and the energy matrix is

$$\left(E(\omega)\right)_{m\mu l\eta} = \left(\omega - \epsilon_{m\mu}\right)\delta_{ml}\delta_{\mu\eta} \tag{5.13}$$

The Σ index on the Greens function means that it is only the tunneling Hamiltonian which is included. The zero on the self energy indicates it is the tunneling self energy.

5.1.1 Self-energy

The Feynman diagram for the tunneling self-energy consists of two tunneling nodes connected by a lead electron propagator. The diagram is shown in figure 5.1. Both the retarded and lesser self-energy need to be found.

The retarded self-energy is defined in (5.12) and agrees with the Feynman diagram. Performing the k-sum gives

$$\begin{aligned}
\Sigma^{r}_{0,m\mu,n\nu}(\omega) &= \sum_{k\alpha\sigma} V^{*}_{m\mu,k\alpha\sigma} G^{0,r}_{k\alpha\sigma}(\omega) V_{k\alpha\sigma,n\nu} \\
&= \sum_{\alpha} \int \frac{d\epsilon}{2\pi} \frac{\Gamma^{\alpha}_{m\mu,n\nu}(\epsilon)}{\omega - \epsilon + ic} \\
&= \sum_{\alpha} \Lambda^{\alpha}_{m\mu,n\nu}(\omega) - \frac{i}{2}\Gamma^{\alpha}_{m\mu,n\nu}(\omega)
\end{aligned} \tag{5.14}$$

where $\Lambda^{\alpha}_{m\mu,n\nu}$ is the principal part of the integral and $\Gamma^{\alpha}_{m\mu,n\nu}(\epsilon)$ is the level width function defined in (4.9). The diagonal part of Λ leads to a shift in the energy spectrum of the quantum dot. This shift is assumed to be included in the level energies ($\epsilon_{m\mu}$) of the model and the anti-diagonal components

are taken to zero.[1]

The lesser self-energy is found from the Feynman diagram (fig. 5.1). Assume that the diagram is for the contour ordered Green's function. The only contour object in the diagram is the lead electron propagator. This means that the expression can be directly translated to the lesser function. Again the k-sum gives

$$\begin{aligned}\Sigma^{<}_{0,m\mu,n\nu} &= \sum_{k\alpha\sigma} V^{*}_{m\mu,k\alpha\sigma} G^{0,<}_{k\alpha\sigma}(\omega) V_{k\alpha\sigma,n\nu} \\ &= \sum_{\alpha} \int \frac{d\epsilon}{2\pi} \Gamma^{\alpha}_{m\mu,n\nu}(\epsilon) \left(i f_{\alpha}(\epsilon) \delta(\omega - \epsilon) \right) \\ &= i \sum_{\alpha} \Gamma^{\alpha}_{m\mu,n\nu}(\omega) f_{\alpha}(\omega)\end{aligned} \tag{5.15}$$

where $f_\alpha(\epsilon)$ is the Fermi distribution of the α-lead.

5.1.2 Non-interacting trace formula

All the unknown functions in the trace formulas in section 4.2.1 have now been found in the non-interacting model, so the final formulas for the electric current and the spin torque can be determined.

Electric current

Using the results (5.14) and (5.15) it is found that

$$\bar{\mathbf{\Sigma}}^{<}_{0}(\omega) + f_{\alpha}(\omega) \bar{\mathbf{\Sigma}}_{0}(\omega) = i \bar{\mathbf{\Gamma}}^{\bar{\alpha}}(\omega) \left(f_{\bar{\alpha}} - f_{\alpha} \right) \tag{5.16}$$

Inserting into (4.15) the expression for the electric current is found

Electric current through a non-interacting quantum dot

$$J^{\alpha}_{e} = \frac{e}{\hbar} \int \frac{d\omega}{2\pi} \mathrm{Tr}_{n,s} \left[\bar{\mathbf{\Gamma}}^{\alpha}(\omega) \bar{\mathbf{D}}^{r}_{\Sigma}(\omega) \bar{\mathbf{\Gamma}}^{\bar{\alpha}}(\omega) \bar{\mathbf{D}}^{r}_{\Sigma}(\omega) \left(f_{\alpha}(\omega) - f_{\bar{\alpha}}(\omega) \right) \right] \tag{5.17}$$

where $\bar{\alpha}$ means the opposite lead than α. This formula for the current will be analyzed in chapter 7 for specific configurations of the magnetizations .

[1] We will later take the wide band limit (section 7.1.1) where Γ is independent of the energy. Hence Λ vanish.

Spin torque

The rather complicated spin torque formula (4.17) simplifies somewhat in the non-interacting case. Inserting the expression for the lesser self-energy (5.15) into (4.17) the expression for the spin torque is found after some algebra

$$\tau_i = \frac{1}{4}\int \frac{d\omega}{2\pi}\mathrm{Tr}_{n,s}\bar{\mathbf{T}}_i \tag{5.18}$$

$$\begin{aligned}\bar{\mathbf{T}}_i = &\left(\frac{1}{2}\bar{\mathbf{D}}^a_\Sigma(\omega)\Big(\bar{\mathbf{\Gamma}}_{principal} + \bar{\mathbf{\Gamma}}(\omega)\sigma_i + \sigma_i\bar{\mathbf{\Gamma}}(\omega)\Big)\bar{\mathbf{D}}^r_\Sigma(\omega)\right.\\ &\left. - i\Big(\sigma_i\bar{\mathbf{D}}^r_\Sigma(\omega) - \bar{\mathbf{D}}^a_\Sigma(\omega)\sigma_i\Big)\right)\\ &\times\left(\big(\bar{\mathbf{\Gamma}}^\alpha + \bar{\mathbf{\Gamma}}^{\bar\alpha}\big)\big(f_\alpha + f_{\bar\alpha}\big) + \big(\bar{\mathbf{\Gamma}}^\alpha - \bar{\mathbf{\Gamma}}^{\bar\alpha}\big)\big(f_\alpha - f_{\bar\alpha}\big)\right)\end{aligned} \tag{5.19}$$

$$\bar{\mathbf{\Gamma}}^i_{principal} = 2iP\int\frac{d\epsilon}{2\pi}\frac{\bar{\mathbf{\Gamma}}(\epsilon)\sigma_i - \sigma_i\bar{\mathbf{\Gamma}}(\epsilon)}{\epsilon-\omega} \tag{5.20}$$

The spin torque is a sum of two factors. One depends on the potential difference of the contacts and one which is independent on this difference. The physical interpretation of the terms will be discussed later. First the common prefactor is simplified. Collecting terms with the factors $\sigma_i D^r$ and $D^a\sigma_i$ gives

$$i\bar{\mathbf{D}}^a_\Sigma(\omega)\Big(\bar{\mathbf{\Gamma}}^i_{principal} + \big(\bar{\mathbf{D}}^0(\omega)\big)^{-1}\sigma_i + \sigma_i\big(\bar{\mathbf{D}}^0(\omega)\big)^{-1}\Big)\bar{\mathbf{D}}^r_\Sigma(\omega) \tag{5.21}$$

The bare dot-Green's functions are diagonal and the expression is easily evaluated. Inserting this into (5.19) gives the final torque formula

Spin torque in the non-interacting quantum dot

$$\tau_i = \frac{1}{4}\int \frac{d\omega}{2\pi}\mathrm{Tr}_{n,s}\bar{\mathbf{T}}_i \tag{5.22}$$

$$\begin{aligned}\bar{\mathbf{T}}_i = &i\bar{\mathbf{D}}^a_\Sigma(\omega)\left(\bar{\mathbf{S}}_i + \bar{\mathbf{\Gamma}}^i_{principal}\right)\bar{\mathbf{D}}^r_\Sigma(\omega)\\ &\times\left(\big(\bar{\mathbf{\Gamma}}^\alpha + \bar{\mathbf{\Gamma}}^{\bar\alpha}\big)\big(f_\alpha + f_{\bar\alpha}\big) + \big(\bar{\mathbf{\Gamma}}^\alpha - \bar{\mathbf{\Gamma}}^{\bar\alpha}\big)\big(f_\alpha - f_{\bar\alpha}\big)\right)\end{aligned} \tag{5.23}$$

$$\bar{\mathbf{S}}_x = \mathrm{Tr}_s\left[\bar{\mathbf{E}}_\omega\right]\sigma_x \tag{5.24}$$

$$\bar{\mathbf{S}}_y = \mathrm{Tr}_s\left[\bar{\mathbf{E}}_\omega\right]\sigma_y \tag{5.25}$$

$$\bar{\mathbf{S}}_z = 2\bar{\mathbf{E}}_\omega\sigma_z \tag{5.26}$$

$$\bar{\mathbf{\Gamma}}^i_{principal} = 2P\int\frac{d\epsilon}{2\pi}\frac{\bar{\mathbf{\Gamma}}(\epsilon)\sigma_i - \sigma_i\bar{\mathbf{\Gamma}}(\epsilon)}{\epsilon-\omega} \tag{5.27}$$

The spin torque has two contributions. One stems from the voltage bias of

the contacts and therefore reflects spin that is deposited on the quantum dot by the electric current. The other one is independent on the potential difference and is due to the difference in magnetizations of the regions. This is thus an equilibrium spin-current, which is well-known from interfaces between non-collinear ferromagnets [34]. In the case where the magnetization is the same in all the regions the prefactor vanishes. This is easily seen for the x- and y- components. Here the σ_i can be extracted from the principal integral due to the diagonal structure of the $\bar{\Gamma}$. Hence the prefactor is a product of some diagonal matrices and an antidiagonal Pauli matrix. This product will have zeros on the diagonal. The z-component will also vanish by direct calculation.

CHAPTER 6

Quantum dot with Coulomb interaction

In this chapter the Coulomb interacting quantum dot is discussed. The Coulomb interaction will generate many-particle corrections to the dot Green's function and self-energies. In general if there are n levels in the dot the interaction will generate corrections involving n particles - n-particle functions[1]. The equation of motion method can be used to find these functions, but this is not the approach we will use.

When a quantum dot is in the Coulomb blockade regime it is only a few levels which contribute to the current through the system. The levels with energies below the conducting ones will contribute with a electrostatic potential which can be incorporated into the level energies of the model. To make things simple we will assume that there is only a single spin split conducting level. THis is reasonable if the levels are distributed wide enough that there is only one spin split level per Coulomb peak.

The chapter begins with a short discussion of the Coulomb Hamiltonian and continues with the derivation of the dot Green's function. In this derivation a Hartree-Fock approximation will be used to decouple the lead and dot operators. Then the large Coulomb interaction limit is taken and the Green's function is found. The retarded self-energy can be determined but the lesser Green's function has to be approximated by the Ng approximation [28] before the Coulomb trace formula is found. This approach is similar to those used in [24] and [33].

[1] If the leads were interacting there would be generated even higher particle functions.

6.1 Coulomb interaction

To describe the Coulomb interaction we will use the constant interaction model [1]

$$H_{Coul} = \frac{U}{2}\sum_{\mu} n_{\bar{\mu}} n_{\mu} \tag{6.1}$$

where $n_\mu = d_\mu^\dagger d_\mu$ is the occupation operator and U is the strength of the Coulomb interaction. The bar over the μ means the opposite spin as μ. The diagonal term is sometimes included but only gives an extra electrostatic potential.

6.2 Dot-Green's function with Coulomb interaction

The calculation of the dot-Green's function follow the same equation of motion technique as in the chapter 5. First the single particle corrections is found and afterward the many-particle contributions are discussed. In all the calculations the commutator relations which are described in the appendix B.1 have been used.

6.2.1 Single particle corrections

The time derivative of the QD-Green's function is the same as in (5.1)

$$i\partial_t D^r_{\mu,\nu}(t-t') = \delta(t-t')\delta_{\mu\nu} + (-i)\theta(t-t')\left\langle\left\{-[H;d_\mu](t);d_\nu^\dagger(t')\right\}\right\rangle \tag{6.2}$$

where the commutator here can be separated into three terms (instead of two when the Coulomb interactions have bee turned off)

$$[H;d_\mu] = [H_0^{QD};d_\mu] + [H_T;d_\mu] + [H_{Coul};d_\mu] \tag{6.3}$$

The first two terms give as in (5.3) and (5.4)

$$[H_0^{QD};d_\mu] = -\epsilon_\mu d_\mu \tag{6.4}$$

$$[H_T;d_\mu] = -\sum_{k\alpha\sigma} V^*_{\mu,k\alpha\sigma} a_{k\alpha\sigma} \tag{6.5}$$

The Coulomb commutator is found by using the (B.8) relation

$$\begin{aligned}[H_{Coul};d_\mu] &= \frac{U}{2}\sum_{\substack{\eta\nu\\ \eta\neq\nu}}[n_\eta n_\nu;d_\mu] \\ &= -U\sum_{\mu} n_{\bar{\mu}} d_\mu\end{aligned} \tag{6.6}$$

These commutators inserted into (6.2) gives

$$(\omega - \epsilon_\mu) D^r_{\mu,\nu}(\omega) = \delta_{\mu\nu} + \sum_{k\alpha\sigma} V^*_{\mu,k\alpha\sigma} F^r_{k\alpha\sigma,\nu}(\omega) + U \sum_{\substack{\eta \\ \eta\neq\mu}} C^r_{\eta\eta\mu,\nu}(\omega) \tag{6.7}$$

where F^r is the tunnelling Green's function from (5.6) and C^r is the new two-particle Green's function both defined below. The definition of the two-particle Green's function is a bit more general than the one generated in (6.6) where the first and second operators have different quantum numbers.

$$F^r_{k\alpha\sigma,\nu}(t-t') = -i\theta(t-t') \left\langle \left\{ a_{k\alpha\sigma}(t); d^\dagger_\nu(t') \right\} \right\rangle \tag{6.8}$$

$$C^r_{\bar\mu\bar\mu\mu,\nu}(t-t') = -i\theta(t-t') \left\langle \left\{ d^\dagger_{\eta'} d_\eta d_\mu(t); d^\dagger_\nu(t') \right\} \right\rangle \tag{6.9}$$

The tunnelling Green's function is found the same way as in the non interacting case giving the result (5.9).

$$(\omega - \epsilon_{k\alpha\sigma}) F^r_{k\alpha\sigma,\nu}(\omega) = \sum_{\mu'} V_{k\alpha\sigma,\mu'} D^r_{\nu',\nu}(\omega) \tag{6.10}$$

6.2.2 Many particle corrections

The Coulomb interaction generated a two-particle Green's function (6.9). This would repeat itself in the general case, but here there are only two levels. Hence only interaction between two particles can occur. The tunnelling Hamiltonian will generate new kinds of two-particle functions by replacing dot operators with lead operators.

The time derivative

The time derivative of the general two-particle Green's function from 6.9 is

$$\begin{aligned} i\partial_t C^r_{\bar\mu\bar\mu\mu,\nu}(t-t') =& \delta(t-t') \left\langle \left\{ d^\dagger_{\bar\mu} d_{\bar\mu} d_\mu(t); d^\dagger_\nu(t') \right\} \right\rangle \\ &+ (-i)\theta(t-t') \left\langle \left\{ i\partial_t (d^\dagger_{\bar\mu} d_{\bar\mu} d_\mu(t)); d^\dagger_\nu(t') \right\} \right\rangle \end{aligned} \tag{6.11}$$

The second term - the time derivative inside the anti-commutator gives rise to three terms. One comming from the non-interacting (bare) dot-Hamiltonian, one appearing from the Coulomb Hamiltonian and finally one originating from the tunnelling Hamiltonian.

The same time anticommutator term

The expectation value of the anticommutator can be evaluated directly. This is due to the delta-function that makes all the operators to be taken at the same time. The diagonal and anti-diagonal terms are determined separately:

Diagonal$\mu = \nu$

$$\left\langle \left\{ d^\dagger_{\bar{\mu}} d_{\bar{\mu}} d_\mu ; d^\dagger_\mu \right\} \right\rangle = \langle n_{\bar{\mu}} \rangle \tag{6.12}$$

Antidiagonal$\mu \neq \nu$

$$\left\langle \left\{ d^\dagger_{\bar{\mu}} d_{\bar{\mu}} d_\mu ; d^\dagger_{\bar{\mu}} \right\} \right\rangle = \langle -d_{\bar{\mu}} d_\mu \rangle \tag{6.13}$$

This means that the same time anticommutator term can be written as

$$\left\langle \left\{ d^\dagger_{\bar{\mu}} d_{\bar{\mu}} d_\mu ; d^\dagger_\nu \right\} \right\rangle = \begin{bmatrix} \langle n_\downarrow \rangle & \langle -d_\downarrow d_\uparrow \rangle \\ \langle -d_\uparrow d_\downarrow \rangle & \langle n_\uparrow \rangle \end{bmatrix} = \sigma_y \langle n_{\mu\nu} \rangle \sigma_y \tag{6.14}$$

where σ_y is a Pauli matrix.

The bare Quantum dot term

The term from the bare dot-Hamiltonian is found quickly. Using the commutator relations in the appendix B.9 and B.11 the contribution is calculated

$$[H_0^{QD}; d^\dagger_{\bar{\mu}} d_{\bar{\mu}} d_{m\mu}] = -\epsilon_\mu d^\dagger_{\bar{\mu}} d_{\bar{\mu}} d_{m\mu} \tag{6.15}$$

The Coulomb term

The Coulomb term cannot generate higher particle functions[2]

$$[H_{Coul}; n_{\bar{\mu}} d_\mu] = \frac{U}{2} \sum_\sigma [n_{\bar{\sigma}} n_\sigma ; n_{\bar{\mu}} d_\mu] = -U n_{\bar{\mu}} d_\mu \tag{6.16}$$

The tunnelling term

Finally, the tunnelling term generates a set of new two-particle Green's functions. These are types involving a mix of lead and dot-operators. The tunnelling commutator has two parts.

$$\begin{aligned} [H_T; d^\dagger_{\bar{\mu}} d_{\bar{\mu}} d_\mu] = \sum_{\substack{k\alpha\sigma \\ \mu'}} \Big(& V_{k\alpha\sigma,\mu'} [a^\dagger_{k\alpha\sigma} d_{\mu'} ; d^\dagger_{\bar{\mu}} d_{\bar{\mu}} d_\mu] \\ & + V^*_{\mu',k\alpha\sigma} [d^\dagger_{\mu'} a_{k\alpha\sigma} ; d^\dagger_{\bar{\mu}} d_{\bar{\mu}} d_\mu] \Big) \end{aligned} \tag{6.17}$$

[2] If a greater number of levels is considered this term becomes much more complicated.

The two different commutators give rise to three terms

$$[a^\dagger_{k\alpha\sigma} d_{\mu'}; d^\dagger_{\bar{\mu}} d_{\bar{\mu}} d_\mu] = a^\dagger_{k\alpha\sigma} d_{l\bar{\mu}} d_\mu \delta_{\bar{\mu}\mu'} \tag{6.18}$$

$$[d^\dagger_{\mu'} a_{k\alpha\sigma}; d^\dagger_{\bar{\mu}} d_{\bar{\mu}} d_\mu] = -(d^\dagger_{\bar{\mu}} d_{\bar{\mu}} a_{k\alpha\sigma} \delta_{\mu\mu'} - d^\dagger_{\bar{\mu}} d_\mu a_{k\alpha\sigma} \delta_{\bar{\mu}\mu'}) \tag{6.19}$$

The three terms each introduce a new type of Green's function. The new Green's functions have one of the quantum dot operators replaced by a lead operator - hence their names

$$B^{r,1}_{k\alpha\sigma\mu,\nu}(t-t') = -i\theta(t-t') \left\langle \left\{ a^\dagger_{k\alpha\sigma} d_{\bar{\mu}} d_\mu(t); d^\dagger_\nu(t') \right\} \right\rangle \tag{6.20}$$

$$B^{r,2}_{\mu k\alpha\sigma,n\nu}(t-t') = -i\theta(t-t') \left\langle \left\{ d^\dagger_{\bar{\mu}} a_{k\alpha\sigma} d_\mu(t); d^\dagger_\nu(t') \right\} \right\rangle \tag{6.21}$$

$$B^{r,3}_{\mu k\alpha\sigma,\nu}(t-t') = -i\theta(t-t') \left\langle \left\{ n_{\bar{\mu}} a_{k\alpha\sigma}(t); d^\dagger_\nu(t') \right\} \right\rangle \tag{6.22}$$

The EOM equations for these functions are calculated in the appendix B.2.

6.2.3 Decoupling and Hartree-Fock

In the equations of motions for the B-functions new two-particle functions are generated. This is terms looking like $\left\langle \left\{ a^\dagger_k a_q d_\mu; d^\dagger_\nu \right\} \right\rangle$. We could continue a step further with the equations of motion for these terms. This is not the way we want to proceed. Instead a Hartree-Fock approximation is used

$$\left\langle \left\{ a^\dagger_k a_q d_\mu; d^\dagger_\nu \right\} \right\rangle \simeq \left\langle a^\dagger_k a_q \right\rangle \left\langle \left\{ d_\mu; d^\dagger_\nu \right\} \right\rangle \tag{6.23}$$

$$\left\langle a^\dagger_k a_q \right\rangle \delta_{k,q} = \langle n_k \rangle \tag{6.24}$$

A similiar treatment is used for the terms of the type $\left\langle \left\{ d^\dagger a_k a_q; d^\dagger_\nu \right\} \right\rangle$. Here the approximation eliminates the terms because the lead term has the form $\langle a_k a_q \rangle$ which is zero for non-interacting ferromagnetic leads.

$$\left\langle \left\{ d^\dagger a_k a_q; d^\dagger_\nu \right\} \right\rangle = 0 \tag{6.25}$$

The last type of terms which is not evaluated directly are expectation values consisting of a mixed pair of lead and dot operators.

$$\left\langle a^\dagger d \right\rangle \simeq \langle ad \rangle \simeq 0 \tag{6.26}$$

This approximation scheme is sometimes referred to as the decoupling scheme.

6.2.4 The system of equations

The system of equations of motion is now closed. Collecting the equations (6.7),(6.10),(B.20),(B.29),(B.38) and expressing the EOM for the C^r-function using (6.11),(6.14),(6.15),(6.16),(6.17) we have

$$(\omega - \epsilon_\mu) D^r_{\mu,\nu}(\omega) = \delta_{\mu\nu} + \sum_{k\alpha\sigma} V^*_{\mu,k\alpha\sigma}(\omega) F^r_{k\alpha\sigma,\nu}(\omega) + U C^r_{\mu,\nu}(\omega) \tag{6.27}$$

$$(\omega - \epsilon_{k\alpha\sigma}) F^r_{k\alpha\sigma,\nu}(\omega) = \sum_\mu V_{k\alpha\sigma,\mu}(\omega) D^r_{\mu,\nu}(\omega) \tag{6.28}$$

$$\begin{aligned}(\omega - \epsilon_\mu - U) C^r_{\mu,\nu}(\omega) = \bar{\sigma}_y \langle n_{\mu\nu} \rangle \bar{\sigma}_y - \sum_{k\alpha\sigma} V_{k\alpha\sigma,\bar{\mu}}(\omega) B^{r,1}_{k\alpha\sigma\mu,\nu}(\omega) \\ - \sum_{k\alpha\sigma} V^*_{\bar{\mu},k\alpha\sigma}(\omega) B^{r,2}_{\mu k\alpha\sigma,\nu}(\omega) + \sum_{k\alpha\sigma} V^*_{\mu k\alpha\sigma,}(\omega) B^{r,3}_{\mu k\alpha\sigma,\nu}(\omega)\end{aligned} \tag{6.29}$$

$$\begin{aligned}\Big(\omega - \big(\epsilon_\mu + \epsilon_{\bar{\mu}}\big) + \epsilon_{k\alpha\sigma} - U\Big) B^{r,1}_{k\alpha\sigma\mu,\nu}(\omega) = \\ \sum_\eta V^*_{\eta,k\alpha\sigma} C^r_{\eta\bar{\mu}\mu,\nu}(\omega) + V^*_{\bar{\mu},k\alpha\sigma} n_{k\alpha\sigma} D^r_{\mu,\nu} - V^*_{\mu,k\alpha\sigma} n_{k\alpha\sigma} D^r_{\bar{\mu},\nu}\end{aligned} \tag{6.30}$$

$$\begin{aligned}\Big(\omega - \big(\epsilon_\mu - \epsilon_{\bar{\mu}}\big) - \epsilon_{k\alpha\sigma} - U\Big) B^{r,2}_{k\alpha\sigma\mu,\nu}(\omega) = \\ \sum_\eta V^*_{\eta,k\alpha\sigma} C^r_{\eta\bar{\mu}\mu,\nu}(\omega) + V_{k\alpha\sigma,\bar{\mu}} n_{k\alpha\sigma} D^r_{\mu,\nu}(\omega)\end{aligned} \tag{6.31}$$

$$\big(\omega - \epsilon_{k\alpha\sigma}\big) B^{r,3}_{\mu k\alpha\sigma,\nu}(\omega) = \sum_\eta V_{k\alpha\sigma,\eta} C^r_{\bar{\mu}\bar{\mu}\eta,\nu}(\omega) + V_{k\alpha\sigma,\bar{\mu}} a^\dagger_{k\alpha\sigma} a_{k\alpha\sigma} D^r_{\bar{\mu},\nu} \tag{6.32}$$

Before solving this set of equations, it is interesting to discuss the physical meaning of the different terms. From the previous chapter we know that F^r gives the tunneling self-energy (Σ_0) which is responsible for a change of the first pole in the dot-Green's function (D^r). The first pole is the one encountered in the non-interacting version of the Green's function. The pole originates from the $\delta_{\mu\nu}$ factor in the first equation and the pole is related to phenomena with only a single particle in the dot. The C^r introduces two-particle corrections to the system. These corrections can be divided into two types. The first type is the terms with C^r in the B^r-equations. These give a second pole in the dot Green's function (D^r) related to phenomena with two particles in the dot at the same time. The second type is the terms in the B^r-equations having a D^r function. These give further contributions to the self-energy related to the first pole like the F^r-function. The strength of the poles are determined by the occupation matrix ($\langle n_{\mu\nu} \rangle$).

6.2.5 The large U limit

The system of equations can be solved numerically for a simple geometry of the contacts [33]. Here we will examine the limit $U \to \infty$. In this limit U is assumed large compared to the other energies involves in the system

$$U \gg \epsilon_\mu \, , \, \epsilon_k \, , \, \|t_{\epsilon,\uparrow}|^2 \rho_{\alpha\uparrow}(\epsilon) \tag{6.33}$$

The last quantity is the left up-up level width which sets the scale for the energy as discussed in section 4.3. The quantity also sets the strength of the coupling between the leads and the quantum dot. Therefore this limit means that the coupling is weak compared to the dot Coulomb interaction. That U is greater ϵ_k should be seen in the light that the electrons which gives the greatest contribution to the current are those which have an energy close to the Fermi level of the lead. In thin context the limit means that U is greater than the bandwidth of Γ. The ϵ_μ is usually measured from the mean of the chemical potentials of the contacts. The limit therefore means that the Coulomb energy is greater than the voltage bias. This is because the energy level of the dot needs to be in the vicinity of the gab between the chemical potentials for current to run through the level.

Consider the terms in the system of equations (6.27 - 6.32). The C^r is of order U^{-1} due to the U on the left hand side of the equation. Combining this with the U multiplied on C^r in (6.27), it is seen that only the terms to order one on the right hand side of (6.29) have to be taken into the calculation. B^1 and B^2 are both to order U^{-1} by themselves due to the U on the left hand side of the equations. They can therefore be neglected. The C^r term in the B^3 equation is also of order U^{-1} and is neglected while the D^r term is of order one. This means that only two terms on the right hand side of the C^r equation survive. This is the $\bar{\sigma}_y \langle n_{\mu\nu} \rangle \bar{\sigma}_y$ and the D^r term from the B^3-equation.

The system is now simple to solve

$$\bar{D}^r = \bar{D}^r_{\Sigma U} \left(1 - \bar{\sigma}_y \langle \bar{n} \rangle \bar{\sigma}_y\right) \tag{6.34}$$

where

$$\bar{D}^r_{\Sigma U} = \left(\bar{E}(\omega) - \bar{\Sigma}^r_0 - \bar{\Sigma}^r_3\right)^{-1} \tag{6.35}$$

where $\bar{\Sigma}^r_3$ is the self-energy originating form the $B^r, 3$-equation. This self-energy is determined in the next section.

6.3 Self-energy

6.3.1 The correction to the non interaction self-energy

From the equations (6.29) and (ă6.32) it is found that the $\bar{\Sigma}^r_3$ self-energy has the expression

$$\bar{\Sigma}^r_{3,\mu\nu} = \tilde{\Sigma}^r_{3,\mu\bar{\mu}} \sigma_{x,\mu\nu} \tag{6.36}$$

The $\tilde{\Sigma}^r_{3,\mu\bar{\mu}}$ self-energy is found following the calculation in (5.14)

$$\begin{aligned}\tilde{\Sigma}^r_{3,\mu\nu}(\omega) &= \sum_{k\alpha\sigma} V^*_{\mu,k\alpha\sigma} G^{0,r}_{k\alpha\sigma}(\omega) \langle n_{k\alpha\sigma}\rangle V_{k\alpha\sigma,n\nu} \\ &= \sum_{\alpha} \int \frac{d\epsilon}{2\pi} \frac{\Gamma^\alpha_{\mu,\nu}(\epsilon) \langle n_{\alpha\sigma}(\epsilon)\rangle}{\omega - \epsilon + ic} \\ &= \sum_{\alpha} \Lambda^\alpha_{3,\mu,\nu}(\omega) - \frac{i}{2}\theta(-\omega)\Gamma^\alpha_{\mu,\nu}(\omega)\end{aligned} \tag{6.37}$$

where $\theta(-\omega)$ is the unit step function[3].

6.3.2 Retarded self-energy

The retarded self-energy could be found by rewriting equation (6.34) to the form of the Dyson equation (3.13). The retarded self-energy is then found as the term in between the free and the full dot-Green's functions. We are not going to need the expression of the retarded self-energy, therefore we will not make the derivation here.

6.3.3 Lesser self-energy

The lesser self-energy cannot be found explicitly in this model due to the Coulomb interaction. Therefore we need to apply an approximation. The one used is the approximation proposed by Ng [28]. The approximation assumes that the lesser and greater self-energies can be written as

$$\bar{\Sigma}^< = A\bar{\Sigma}^<_0 \quad , \quad \bar{\Sigma}^> = A\bar{\Sigma}^>_0 \tag{6.38}$$

where A is to be determined by the identity $\Sigma^< - \Sigma^> = \Sigma^r - \Sigma^a$. This will give an expression for the lesser self-energy looking like this

$$\bar{\Sigma}^< = (\Sigma^r - \Sigma^a)(\Sigma^r_0 - \Sigma^a_0)^{-1}\bar{\Sigma}^<_0 \tag{6.39}$$

The assumption that the lesser and greater self-energies can be written on the above form (6.38) with the same A has some nice properties. It is exact in the equilibrium limit ($\mu_L = \mu_R$) and also in the non-interacting limit ($U = 0$) and finally the continuity equation ($J_L = -J_R$) is satisfied in steady state.

6.4 Self consistent solution of $\langle n_\mu \rangle$

The occupation of the levels in the quantum dot are not in general easy to determine and will in the general case have to be calculated self-consistently.

[3] The Heaviside function

In a non-equilibrium system the occupation is given by the lesser-Green's function

$$\langle n_\mu \rangle = i \int \frac{d\omega}{2\pi} D^<_{\mu,\mu}(\omega) \tag{6.40}$$

The occupation have to be calculated self-consistently because it enters in the lesser dot-Green's function. The self-consistent method is where the occupation is first calculated from the non-interacting result. This result is then used to calculate a new occupation. The new occupation is used as basis (start) for the next calculation of the occupation. This procedure is repeated until the resultant occupation is equal (or within a certain accuracy) to the start occupation.

6.5 Coulomb trace formulas

As in the non-interacting model there are a variety of formulations of the GTF. This combined with the different schemes to calculate the lesser function and the occupation number we have some choice in the method used to calculate the current and spin torque. In this light the most general formulas will be presented here and in later chapters the specific calculation methods used there will be discussed.

6.5.1 Current Coulomb trace formula

Inserting the results from this chapter into the symmetric trace formula (4.16) and using our algebraic skills the trace formula for the electric current is found as

Symmetric electric current through a Coulomb interacting quantum dot with Ng approximated lesser dot-function

$$J_e = \frac{-e}{4\hbar} \int \frac{d\omega}{2\pi} \mathrm{Tr}_{n,s} \left[\left(\bar{\Gamma} - \bar{\Gamma}_{corr} \right) \bar{A}(\omega) \right] (f_L - f_R) \tag{6.41}$$

$$\bar{\Gamma}_{corr} = \left(\bar{D}^a \right)^{-1} \bar{\Gamma}^{-1} \left(\bar{\Gamma}_L - \bar{\Gamma}_R \right) \bar{D}^a \left(\bar{\Gamma}_L - \bar{\Gamma}_R \right) \tag{6.42}$$

$$\bar{A}(\omega) = i \left(\bar{D}^r - \bar{D}^a \right) \tag{6.43}$$

$$\bar{D}^r(\omega) = \bar{D}^r_{\Sigma U}(\omega) \left(1 - \bar{\sigma}_y \langle \bar{n} \rangle \bar{\sigma}_y \right) \tag{6.44}$$

$$\langle \bar{n} \rangle = i \int \frac{d\omega}{2\pi} \left(\Sigma^r_0 - \Sigma^a_0 \right)^{-1} \left(\Sigma^r - \Sigma^a \right) \bar{\Sigma}^<_0(\omega) \tag{6.40}$$

The new function $A(\omega)$ is the spectral function of the quantum dot. It will be discussed in detail in chapter 7.

6.5.2 Spin torque Coulomb trace formula

The trace formula for the spin torque can be found by combining the results from the Coulomb Greens function (6.34 and 6.39) with the spin torque formulas (2.29-2.31). Due to lack of time we will not investigate the Coulomb effects on the spin torque further than show that the direct interaction term is zero.

The direct interaction term

This term in the torque equations originated from the time derivative of the spin-occupation operator (2.18). It describes how the interacting part of the Hamiltonian directly influences the torque. In the case of the Anderson Coulomb interaction Hamiltonian this term is zero. The elements of the matrix is the sum of terms with the form $[n_{n\nu}n_{m\mu}; d^\dagger_\eta d_{\eta'}]$. These terms are all zero as can be seen from the commutator relation (B.10).

6.6 Summary of the model chapters

In the previous two chapters two models for the quantum dot have been presented and the current through the system has been found. The two model can be seen as the two limits of the general solution to the system of equations (6.27-6.32). The non-interacting model can be seen as the limit of $U = 0$ (compared to Γ) and the Coulomb model in this chapter was taken to the limit $U \to \infty$. The two models allow for two different kinds of transport. In the $U = 0$ case it is a coherent transport because the electrons are not in the quantum dot long enough to interact. Therefore the only correlation between the electrons are the Fermi algebra[4]. The Coulomb model with $U \to \infty$ only allows a strongly correlated transport. When the electrons move through the quantum dot they can only do so single wise because of the strong Coulomb repulsion.

The general solution of the system of equations (6.27-6.32) will describe the transition from the coherent to the strongly correlated transport.

The effects of the two different transport phenomena are discussed in length in the next chapter.

[4]Pauli's exclusion principle

CHAPTER 7

The current through the quantum dot

When the results from the previous three chapters are combined, we are in a position to discuss the different phenomena which the electric current depend on. The results from the previous chapters are very general in nature and contain many parameters which can be adjusted. To keep the analysis simple we will only use two geometries of the magnetizations in the discussion. This allows us to first describe the basic nature of the system and then turn on other parameters to see how the system reacts.

The chapter starts with a description of the methods used. The equations are put into the linear response regime and the zero temperature limit is taken. Then the properties of the spectral function are presented. The energy and current states of the system are discussed to clarify the behavior of the occupation of the dot levels and the electric current. Both of these are discussed in detail after wards.

7.1 The analysis method

The method we have used to analyze the current formulas is simple. The linear response and zero temperature limits are taken. This is primarily done to be able to isolate the different phenomena from each other and not to have a temperature to smear out the effects. One last reason for making these limits is the fact that an analytical result can be found in the non-interacting model.

The chosen geometries only depend on one angle instead of three in the general case. Furthermore the geometries could be realized experimentally.

Before the results are presented in section 7.5 the properties of the system are discussed to give a reference frame for the interpretation of the current curves.

7.1.1 Linear response

The full response of the system to the voltage bias is found by performing an integral over a product of the trace of the matrices and the difference of the Fermi functions of the leads. If we instead only consider the linear response of the system and take the zero temperature limit the integral vanishes.

The linear response is easily found due the difference of the Fermi functions. Put $\mu_L = \mu + \frac{eV}{2}$ and $\mu_R = \mu - \frac{eV}{e}$ where $\mu_{L(R)}$ is the chemical potential of the left (right) lead, μ is the Fermi level at equilibrium and V is the applied voltage. Expanding the Fermi functions to first order about μ

$$f_L(\omega, \mu_L) - f_R(\omega, \mu_R) = -eV \frac{\partial f(\omega, \mu)}{\partial \omega} \tag{7.1}$$

Here it was used that $f\omega, \mu$ is a function of the difference $\omega - \mu$. The linear response result is only useful if the potential bias is very small. From the above it is seen that the current depend linearly of the voltage. Hence Ohm's law is valid. It is therefore instructive to consider the conductance ($G = \frac{I}{V}$) instead of the current. The prefactor to the integral or trace is the quotient $\frac{e^2}{\hbar}$ which is often described as the quantum unit of the conductance. The quotient has the magnitude $38,7\,\mu S$ and the corresponding resistance $\frac{\hbar}{e^2}$ is $25,8\,k\Omega$.

The self consistent solution of the occupation numbers also simplifies. In linear response, we consider the general trace formula to first order in the non-equilibrium parameter - the voltage bias. The conductivity can therefore be calculated in equilibrium. The occupation in equilibrium can be expressed as [4]

$$\langle n_{\mu\nu} \rangle = \int \frac{d\omega}{2\pi} A_{\mu\nu}(\omega) f(\omega) \tag{7.2}$$

where f is the Fermi function and A_μ is the spectral function defined in (6.43). The spectral function depend linearly on the occupation matrix. Hence the equation (7.2) is a linear equation and the elements of the occupation matrix can be found in terms of the integrals of the entries of the spectral- Fermi function product. When the zero temperature limit is taken the Fermi function becomes a step function and the integrals could in principle be found analytically. In the calculations below the integrals have been found numerically.

Temperatures of the system

A finite temperature is expected to broaden the levels of the dot and thereby give smaller resonances. Therefore it is instructive to examine which phenomena are present at $T = 0$ and then later find their dependence with finite temperatures. In the linear response limit and $T = 0$, the differential quotient in (7.1) becomes a delta function

$$-\frac{\partial f(\omega,\mu)}{\partial \omega} = \delta(\omega - \mu) \tag{7.3}$$

This will collapse the integral and give the GTF a simple form similar to the Landauer-Büttiker [6].

The zero temperature limit should not be considered literally meaning that the temperature is zero Kelvin. Instead it should be seen as the limit where $T \ll \Gamma$, where Γ is the coupling strength.

Wide band limit

The dependence on energy of the level width function $\bar{\Gamma}$ can be neglected if the wide band limit is assumed. In the wide band limit the tunneling matrix ($\bar{\mathcal{T}}$) is assumed to be constant within the conducting band limits. The approximation is valid if the scale on which $\bar{\mathcal{T}}$ typically changes is much larger than the width of the dot Green's function ($\bar{\Gamma}$). This is indeed often true in practice [4].

If we for a short moment turns the attention toward the spin torque formula. This assumption will make the principal value integral vanish in equation (4.17) leaving us with a more simple expression for the torque.

7.1.2 The configurations of the system

The general case with arbitrary angles between the contacts and the magnetization of the quantum dot is very complicated and most of the configurations are not experimentally realizable or at least uncontrollable at the moment. The two simple geometries where the contact magnetizations are either parallel or anti-parallel are used as the basis for the analysis. The quantum dot magnetization is assumed to have a direction which has an angle θ to the parallel direction. The geometries are illustrated in figure 7.1.

The parallel - anti-parallel configurations are experimentally possible and have been used in numerous experiments [13]. The direction of the quantum dot magnetization is more difficult to control but it could be possible using a weak magnetic field perpendicular to the magnetizations of the contacts. As long as the perpendicular field is weak compared to the field needed to change the contact magnetizations, it would be able to manipulate the dot

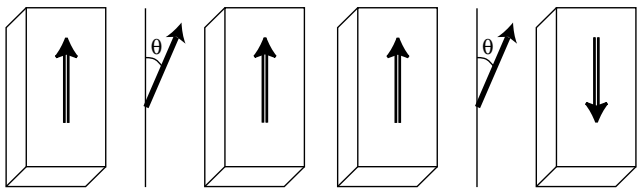

Figure 7.1: The geometry of the parallel and anti-parallel configuration of the contacts and the quantum dot magnetization with an angle θ to the direction of the parallel magnetization.

magnetization direction to some extent. The result is only dependent on the projection of the parallel direction onto the dot direction so this model should cover all the possible dot directions.

The left and right rotation matrices describing this geometry are identical for both the parallel and anti-parallel configurations. In the anti-parallel geometry the tunneling probabilities of the right lead have been rotated with an angle π. This last rotation is in fact the rotation of the magnetization from the parallel to the anti-parallel direction around an axis perpendicular to the parallel direction.

$$\bar{U} = \begin{bmatrix} \cos\left(\frac{\theta}{2}\right) & -\sin\left(\frac{\theta}{2}\right) \\ \sin\left(\frac{\theta}{2}\right) & \cos\left(\frac{\theta}{2}\right) \end{bmatrix} \tag{7.4}$$

$$\bar{\mathcal{T}}_P^L = \bar{\mathcal{T}}_P^R = \bar{\mathcal{T}}_{AP}^L = \begin{bmatrix} 1 & 0 \\ 0 & \gamma \end{bmatrix} \tag{7.5}$$

$$\bar{\mathcal{T}}_{AP}^R = \bar{\sigma}_x \bar{\mathcal{T}}_{AP}^L \bar{\sigma}_x \tag{7.6}$$

In this way, we have complete control of the parameters of interest. θ is the angle from the parallel direction to the dot direction and γ is the polarization of the leads defined in (4.3). Unless otherwise noted the polarization of the contacts are identical.

7.1.3 The energy levels

The energy levels is described by two parameters. A level spacing (a) describing the distance between the two levels. The level spacing is two times the Zeeman energy of the spin splitting. The second parameter is the level energy or gate voltage. It describes the energy difference between the non-split level and the Fermi level of the leads in equilibrium.

7.2 The different states of the system

To understand the physics behind the current graphs, we need to investigate the states of the system. Especially an understanding of the differences

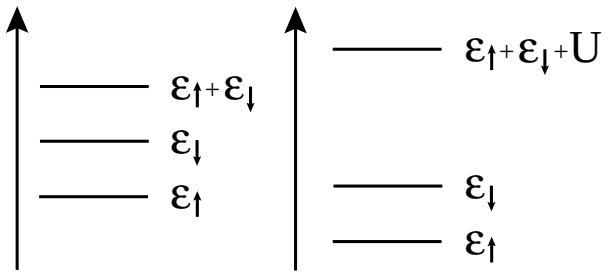

Figure 7.2: The left figure shows the energy states of the non interacting quantum dot while the right shows the energy states of the Coulomb quantum dot. The energy increases the higher the level is placed. $\epsilon_\uparrow$ and $\epsilon_\downarrow$ are the energies defined in section 2.1.3. The two states with the lowest energy are the single occupied quantum dot, while the state with the highest energy is the fully occupied dot. Notice the energy difference between the fully occupied dot in the non interacting and Coulomb dots. This difference is due to the Coulomb repulsion (energy).

between the non interacting - coherent transport and the strong Coulomb - correlated transport phenomena. First the energy states are discussed and then the current states. The latter are very important for the understanding of the current graphs.

7.2.1 Energy states

The single particle energy states were discussed in the presentation of the Hamiltonians of the system. There are two single particle states in the quantum dot. They are the spin up and spin down states with the energies $\epsilon_\uparrow$ and $\epsilon_\downarrow$ respectively. Furthermore there is a two particle state. This state has a different energy depending on the model of the quantum dot.

In the non interacting case the two particle state has the energy $\epsilon_{two} = \epsilon_\uparrow + \epsilon_\downarrow$ while in the Coulomb case it has the energy $\epsilon_{two} = \epsilon_\uparrow + \epsilon_\downarrow + U$. The latter will in the strong Coulomb limit ($U \to \infty$) also go to infinity. This means that it takes an infinite amount of energy to have two particles in the quantum dot at the same time. Hence in the strong Coulomb regime only the single particle states are available for the transport through the dot. The energy states are shown in figure 7.2

7.2.2 Current states

The current states are also different in the coherent and correlated transport regimes. As with the energy states there exists current states with one or two particles. The states to the lowest order in the tunneling coupling are illustrated in figure 7.3.

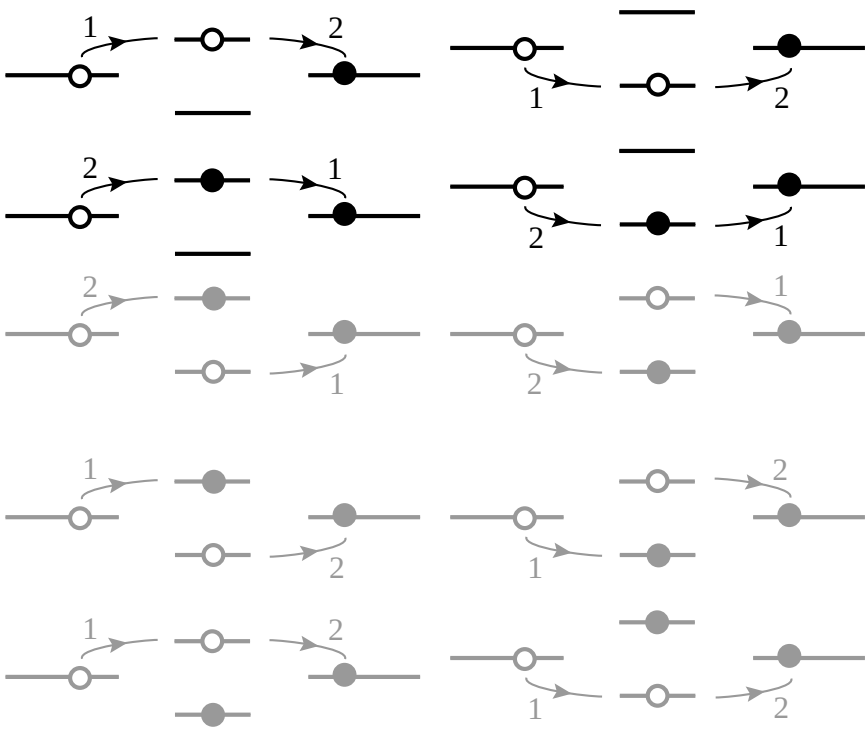

Figure 7.3: The figures illustrate different states (channels). The energy of the levels increases toward the top. The numbers on the lines tell which process occurs first. The illustrations show the processed to the second order in Γ. The two in the first line show the single particle current states. The two following rows are processes where a particle tunnels out of the dot before a second tunnel in. The last four show processes where there are two particles in the dot at the same time. These current states will not contribute in the strongly correlated regime. (The color of the illustrations in the third line should have been black. Therefore neglect the coloring.)

Both the coherent and correlated transport regime have all the single particle current states. All the two particle states contribute to the coherent tunneling but only some contribute to the correlated transport of the strong Coulomb model. This is again due to the infinite Coulomb energy. The two particle states that do contribute are in fact not two particle states in the energy because the two electrons involved in the tunneling are not in the dot at same time. Instead the electron from the left lead has to wait until the electron on the dot tunnels out to the right lead before it can enter the dot. Hence the name correlated transport.

7.3 The spectral function

The spectral function[1] is a very important quantity in many particle physics. Here it surfaced in the trace formulas where the current can be written as the trace of a corrected level width function and the spectral function. The diagonal terms of the spectral function matrix have a physical interpretation. They can be shown to be non-negative using the Lehmann representation and the integral of one of the diagonal term over all frequencies is one [21]. Hence the diagonal terms can be interpreted as a probability function.

In this system the spectral function can be seen as the energy resolution for a particle in a state in the quantum dot. This means that if we want to create an excitation of the dot with the energy ω the spectral function $A_{\mu\mu}$ tells us the probability for this to happen by adding a particle in the quantum dot state μ. The broadening of the spectral functions are due to the non zero self-energies.

7.3.1 The spectral functions of the system

The spectral functions of the system depend on the model. Some of the spectral functions are shown in figure 7.4. In the non interacting case it has two peaks one for each of the levels of the dot. One centered on the energy $\epsilon_\uparrow$ and one centered on the energy $\epsilon_\downarrow$. The broadening of the peaks depend on the angle (θ) because of the difference in directions of magnetizations of the regions.

The Coulomb spectral function also has the two peaks at $\epsilon_\uparrow$ and $\epsilon_\downarrow$. Furthermore it has two peaks situated around $\epsilon_\uparrow + U$ and $\epsilon_\downarrow + U$. These correspond to the energy needed to excite the dot by putting a second particle into the dot. In the strong Coulomb regime these two particle peaks will be put at infinity. This means that they will not contribute to the current but they will still contribute with a finite weight to the probability integral. Therefore the single particle Coulomb peaks have a lesser probability weight than the non-interaction peaks. This decrease of the probability weight depends on the angle.

7.3.2 The current integral

Before continuing with the analysis of the system it is instructive to consider the difference between the linear to the full response regimes and the zero temperature limit.

The linear response is from the earlier derivation (7.1) the linear term when the current formula is expanded in the bias potential. This combined with

[1] Also called the spectral density function

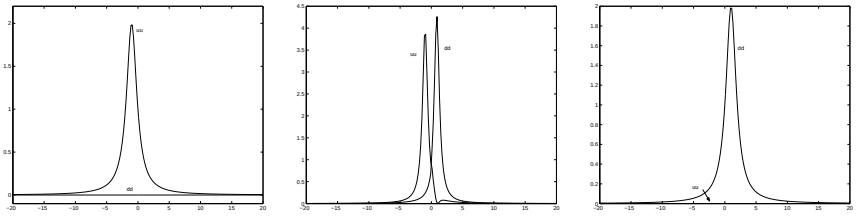

Figure 7.4: The diagonal spectral functions of the parallel coherent system. The level energies are symmetric around the Fermi level (a=1). The left figure is for $\theta = 0$, the middle one for $\theta = \frac{\pi}{2}$ and the right one is for $\theta = \pi$. The two functions shown are the two diagonal components of the spectral function matrix. The up-up spectral function in the right figure seems to be zero, but in fact it is a delta function with the peak at $a = -1$. The the unit of the x-axis is energy.

the zero temperature limit gives that the current integral is determined from the spectral function values at $\omega = 0$. These values together with the Γ-matrix determine the conductivity.

In the general case but still in zero temperature the current is a function of the weight of the spectral functions between the left and right chemical potentials. This is because of the fact that the Fermi functions become step functions in the zero temperature limit. The weight of the spectral functions are then multiplied by a Γ-matrix to give the right mixing of the up and down contributions according to the spin valve effect. This is of course under the wide band limit assumption.

When the temperature is finite, the calculations follow the ones in the zero limit. The main difference is due to the Fermi functions. They are no longer step functions and that means that a wider range of the spectral functions contribute compared to the sharp boundaries in the zero temperature case.

The interference effects which occur are most clearly seen in the linear response regime. This is because the effects only depend on the values of the spectral functions at $\omega = 0$. In the other regimes a larger part of the spectral functions contribute. Hence the fine resonances are smeared out

7.4 The occupation of the quantum dot

In linear response the occupation is determined by the part of the spectral function where ω is negative (7.2). The occupation of the two levels depends primarily on two things. The energy of the level compared to the Fermi energy. If the level energy is less than the Fermi energy, it is favorable for the system to have the level occupied. If the level energy is greater it is of course less favorable. Even if the peak is centered above the Fermi energy it

can still contribute due to its finite width. The width is determined by the angle and we will see how the levels become fully filled or depleted as the angle varies.

7.4.1 Dependence on the level energies

The occupation is very sensitive to the energies of the levels. If a level has an energy that are lower than the equilibrium Fermi energy it is favorable for the system to have the level occupied in an attempt to minimize the energy of the system. The opposite is true if the level has an energy that is greater than the Fermi energy.

When a current is passed through the system the occupations change. The change depends upon the current that passes through the respective levels. Hence if the current is passed through a single level we could expect the occupation to decrease while the occupation of the other level would coincide with the equilibrium occupation. This is clearly seen in figure 7.5. Here the occupations are shown as a function of the angle. Both the coherent and correlated occupations are shown in the left figure. In that figure the energy levels are symmetric about the Fermi energy with the spin up level with the lowest energy. The right figure shows how the parallel correlated occupation depends on the gate energy. The level spacing is $a = 1$. The illustrated situation shows how the occupation decreases as the up level passes the Fremi level.

Considering the parallel configuration, it is seen that the occupation of the up level is greater than the down level as expected considering the level energies. The occupation shows the expected dependence on the angle. At $\theta = 0$ the current can only pass through the up-level and the occupation of the level is at its lowest. When $\theta = \pi$ the current cannot pass through the up level because the up-electrons from the leads see the level as a down level due to the difference in spin basis. This means that the level is always occupied due to its energy that is below the Fermi energy. The occupation shows the same behavior. A $\theta = 0$ the level is unoccupied because current cannot run through the level and the level has a greater energy that the Fermi energy. At $\theta = \pi$ the current only runs through the down level giving it a finite occupation.

In the strong Coulomb limit the occupation is lower that in the non interacting model. This is because the the strong repulsive Coulomb interaction makes sure that there can only be a single particle in the dot at a time. Due to the lower energy the particle is sitting in the up state and thereby giving a zero occupation of the down state.

The anti-parallel configuration shows no angular dependence. This is because the self-energies are diagonal and independent on the angle in this configuration. This is because the system does not have a preferred spin basis due to the symmetric but opposite contacts.

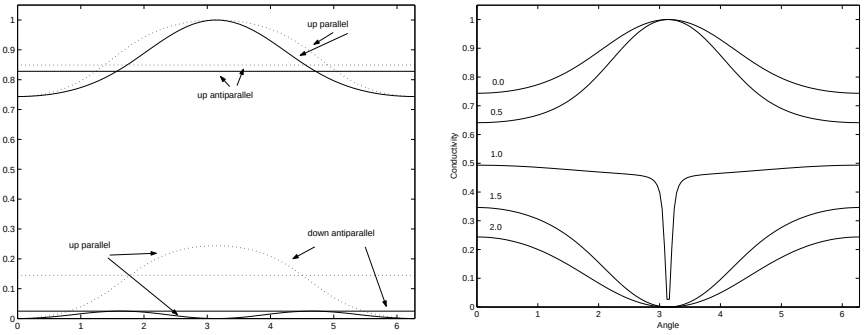

Figure 7.5: The left figure shows the parallel and antiparallel, coherent and correlated occupations for a level spacing of $a = 1$ with the levels symmetric around the Fremi level. The dotted lines are the coherent occupations. The right figure figure shows how the up-up occupation in the parallel correlated regime depends on the gate energy. The numbers on the graph are the gate energies

7.5 The current through the system

To remember the differences in the current formulas, they will be summarized here. The non interacting GTF equation could be solved exactly. (5.17) simplifies with the help of (7.1) and (7.3) to the conductivity GTF

$$G = \frac{e^2}{\hbar}\mathrm{Tr}_{n,s}\left[\bar{\mathbf{\Gamma}}^{\alpha}(\omega)\bar{\mathbf{D}}^{r}_{T}(\omega)\bar{\mathbf{\Gamma}}^{\bar{\alpha}}(\omega)\bar{\mathbf{D}}^{r}_{T}(\omega)\right] \tag{7.7}$$

In the derivation of the Coulomb formula we were not that lucky, but in the parallel geometry we can assume a proportionate coupling and thereby eliminate the troublesome lesser term in the trace formula and find a simple expression for the parallel conductivity.

$$C_P = -\mathrm{Tr}\left[\bar{\Gamma}^{L}\mathbf{IM}\left[\bar{D}^{r}\left(0\right)\right]\right] \tag{7.8}$$

The anti-parallel formula is more cumbersome. Using the Ng approximation (6.39) the conductivity in the zero temperature linear response regime can be expressed as

$$C_A = -\frac{1}{4}\mathrm{Tr}\left[\mathbf{IM}\left[\bar{D}^{r}(0)\right]\left(\bar{\Gamma} - \bar{\Gamma}_{corr}(0)\right)\right] \tag{7.9}$$

$$\bar{\Gamma}_{corr}(0) = \left(\bar{\Gamma}^{L} - \bar{\Gamma}^{R}\right)\left(\bar{D}^{a}(0)\right)^{-1}\bar{\Gamma}^{-1}\left(\bar{\Gamma}^{L} - \bar{\Gamma}^{R}\right)\bar{D}^{a}(0) \tag{7.10}$$

In order to calculate the parallel and anti-parallel conductivities the occupation numbers have to be determined self consistently as discussed in section 7.1.1.

In the following the leads will be assumed to be symmetric and half metals ($\gamma = 0$). This is done to enhance the resonance effects which are weakened by a finite polarization. This is shown later in section 7.5.2.

7.5.1 The interference of the paths

The coherent transport of the non-interacting model is analyzed first. The conductivities can be found analytically and the result is very interesting:

$$G_P = \frac{e^2}{\hbar}\frac{\cos\theta^2}{a^2+\cos\theta^2} \tag{7.11}$$

$$G_{AP} = \frac{e^2}{\hbar}\frac{16a^2\sin\theta^2}{(1+a^2)^2} \tag{7.12}$$

Here $a = \frac{\epsilon}{\Gamma}$. The parallel conductivity has the form of a Breit-Wigner line shape [27]. It is a big surprise that the parallel conductivity is zero for an angle of $\frac{\pi}{2}$ and . This zero is due to destructive interference between the two paths through the spin up and spin down levels of the dot. There are two effects which could be responsible for this interference. Either it is the change of bases or the process of multiple in and out tunneling of the dot. Using the bare dot-Green's functions instead the tunneling dot-Green's functions this can be examined because it eliminates the multiple in- and out-tunneling corrections. In other words it can be seen as the conductivity to the second order in Γ.

$$G_P^{\Gamma^2} = \frac{e^2}{\hbar}\frac{\cos\theta^2}{a^2} \tag{7.13}$$

$$G_{AP}^{\Gamma^2} = \frac{e^2}{\hbar}\frac{\sin\theta^2}{a^2} \tag{7.14}$$

It is seen that the zero resonance remains and we can conclude that the resonance is due to the change of basis in the tunneling process and not to interference between multiple in and out tunneling of the dot. We can also see that the inclusion of the in and out self-energy in the Green's functions the divergence for $a = 0$ in (7.13) is lifted. The zero resonance is seen to be robust to the tunneling processes which is interesting and rarely seen.

Other interesting properties of the parallel conductivity is the symmetry ($\theta = \pi - \theta$) of the angle about $\theta = \frac{\pi}{2}$. This is due to fact that when the angle is greater than $\frac{\pi}{2}$ the current is led through the other spin level.

When a is zero the dot no longer has a preferred spin basis and the in-tunneling electrons keep their bases. This is seen in the parallel conductivity which is equal to $\frac{e^2}{\hbar}$ and independent of the angle and it is seen in the anti-parallel conductivity which is zero. The last case is when an electron tunnel in from the left contact and keeps its basis its overlap with the up-spin state in the right contact is zero.

The line shape of the anti-parallel conductivity is a squared Lorentzian of a weighted by $16\sin(\theta)$. The angular dependence was seen in (7.13) to originate solely from the change of basis tunneling process while the Lorentzian shape is from the in-and-out tunneling processes. It has maximum for $\theta = \frac{\pi}{2}$

which is expected because here the dot direction is precisely in between the contact direction and therefore maximizes the overlap of the states. It is zero when the direction is parallel to one of the contacts and thereby eliminates the overlap with the other contact.

The dependence on the level spacing is very different between the parallel and anti-parallel geometries. The parallel conductivity has maximum for $a = 0$ where both spin channels are fully opened and the angular dependence is non existent. For a finite a the zero resonance blinks into existence and is broadened as a increases. The maximum conductivity is for $\theta = 0$ and $\theta = \pi$ with the value $\frac{1}{1+a^2}$. The reason for the decrease in conductivity is that the levels of the dot get further and further away from the energy levels of the contacts and that the overlaps drop. The anti-parallel conductivity is zero for $a = 0$, maximal for $a = 1$ and decreases for larger a.

7.5.2 Coherent vs. correlated tunneling

When the Coulomb interaction is turned on the resonance discussed in previous section changes. First it is found how the conductivities depend on the level spacing when the levels are symmetrically around the Fermi level. Next the dependencies on the gate voltage is examined and lastly the dependence on the polarization of leads is found.

The level spacing dependence of the current

The main difference between the non-interacting and the strong Coulomb dot is the blocking of the current states which involves two particles in the dot at the same time. This effect is responsible for the elimination of the peak around $\theta = \pi$. This is seen in top part of figure 7.6 where the conductivities for both regimes are shown in the parallel configuration. The graphs are for symmetric levels around the Fermi level with different level spacing. The resonance form the coherent regime seems to have vanished. This is because the path through the down level is closed and no interference is possible. When zooming in on the valley around π on the correlated graphs for level spacing greater than $a = 1$ there seems to be some structure of order $10^{-3}\frac{e^2}{\hbar}$. Whether this structure is due to numerical problems or an artifact of the strong Coulomb limit is not know.

The conductivities for the different level spacings in the anti-parallel configuration are shown in the bottom part of figure 7.6. The conductivity is less in the correlated regime than in the coherent regime. This is not unexpected because the strong Coulomb interaction closes the current through one of the levels. The peaks of the curves for level spacings 1.0 and 3.0 are slightly shifted toward $\theta = 0$ while the curve for the level spacing 0.01 is shifted toward $\theta = \pi$. These shifts might seem strange but we have to remember

that the anti-parallel configuration has no preferred direction. Hence the position of the peak for a curve is very difficult to predict.

The gate dependence of the current

When the level spacing is kept fixed on $a = 1$ and the gate[2] is swept between -1.5 and 2.0. This range allows us to examine currents behavior as the levels are moved a position where they both are under the Fermi level to a position where they are both above the Fermi level. The program was not able to give results when the energy levels were exactly at the Fermi level because of singular matrices. Therefore at the instances where this occur a small amount (10^{-3}) is added to the level energy.

The behavior of the coherent current in the parallel configuration is show in figure 7.7. It is seen how the current depends on the spin valve. When the down level pass the Fermi level the current primarily runs through that level and vice versa when the up level passes. Furthermore, it is seen how the angle at which the zero resonance occur depend on the energy levels. The resonance exists as long as the Fermi level is in between the two spin levels but the resonance is pushed away from the level closed to the Fermi level. This is because the level which is closer has a larger amount of current passing through and thereby a greater weight in the interference.

The gate dependence of the correlated conductivity is shown in figures 7.8. Here it is seen that the Coulomb interaction eliminates the contributions to the current originating from the down level. The dip in the graph for $gate = 1.0$ should go to zero. It does not because the level is raised a small amount above the Fermi level due to numerical problems discussed in the beginning of the section. When both levels are above the Fermi level current can pass through both levels because it is no longer energetically favorable to have the up level occupied.

In figure 7.9 it is seen that the coherent transport through the anti-parallel configuration is independent on which of the levels that is closest. It only depends on the the energies of the levels and not on which spin the level has. The current is invariant under the spin interchange operator! This is because in the anti-parallel configuration the system do not have a preferred spin basis. The current has its maximum for the angle $\frac{\pi}{2}$. This is because both levels contribute equally here. If we considered asymmetric couplings the maximum would move toward the lead with the largest coupling.

In figure 7.10 is the correlated conductivities are shown. There seems to be a strange behavior of the graphs, but as mentioned above we have to remember

[2]The gate is here used about the midpoint of the level energies. This means that the level energies have an energy of $\pm a$ around the value of the gate. Then the gate is zero it corresponds to the case discussed above where the levels lie symmetric around the Fermi level.

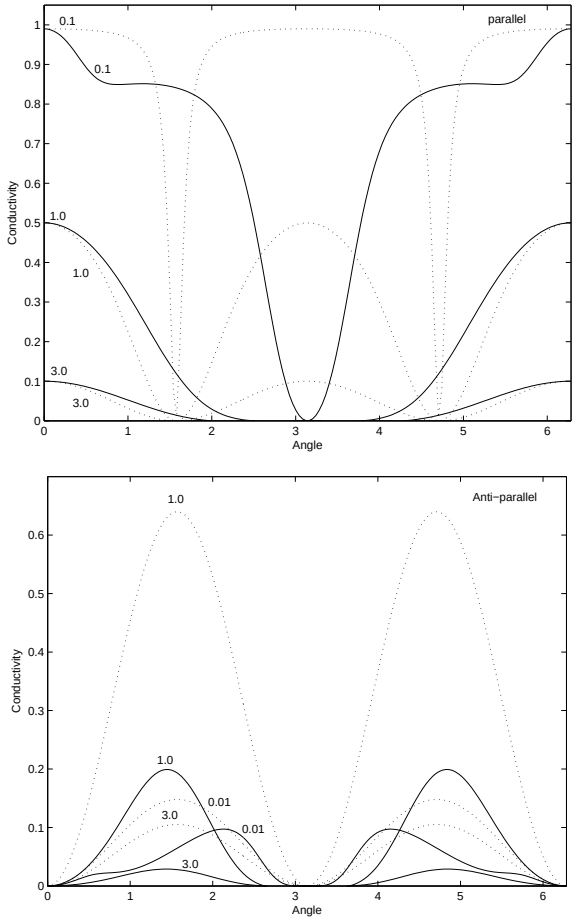

Figure 7.6: The level spacing dependence of the conductivity. The full lines are the correlated conductivities and the dotted lines are the coherent conductivities. The top figure is in the parallel configuration and the bottom one is in the anti-paralle configuration. The numbers on the curves are the level spacing The y-axis is in units of $\frac{e^2}{\hbar}$

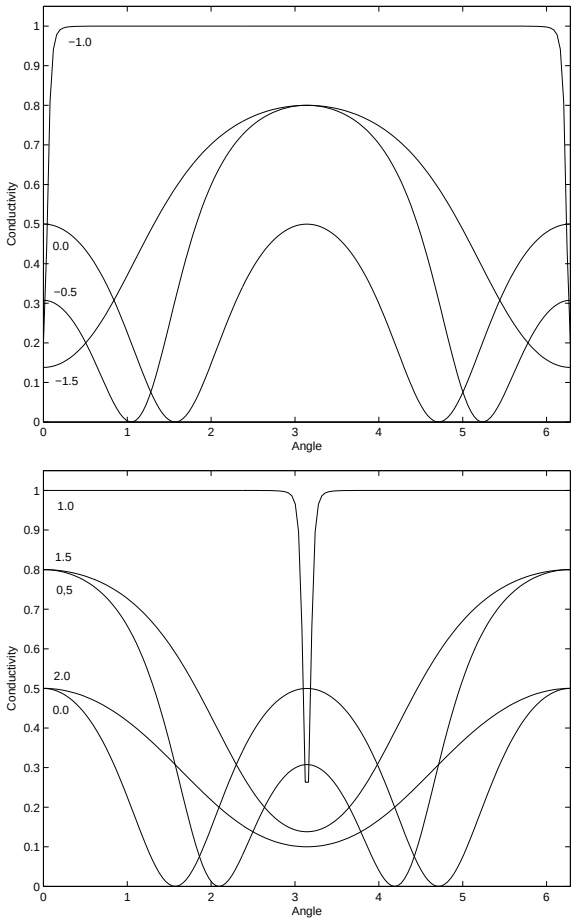

Figure 7.7: The gate dependence of the parallel coherent conductivity. The top figure shows the gates from -1.5 to 0.0 while the bottom figure shows the gates from 0.0 to 2.0. The numbers on the graphs is the gate energy. The y-axis is in units of $\frac{e^2}{\hbar}$

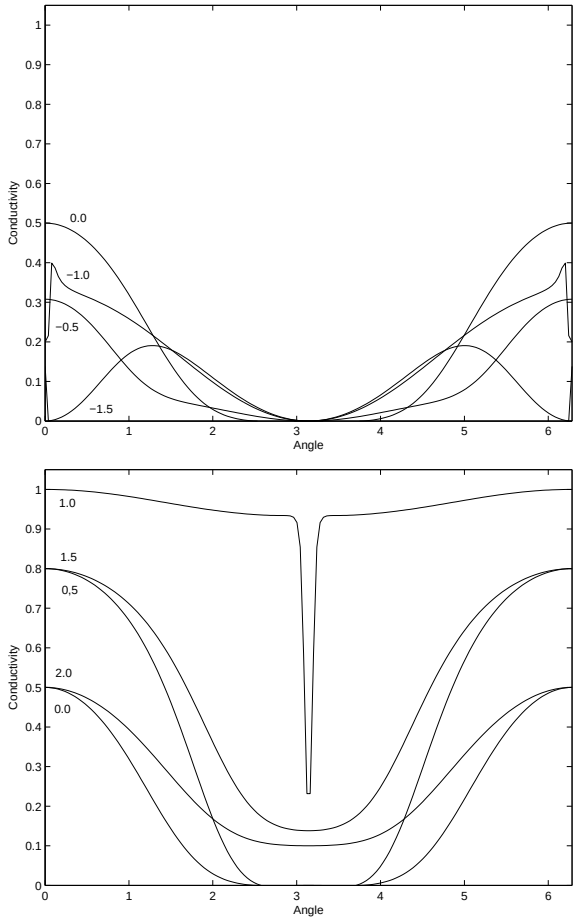

Figure 7.8: The gate dependence of the parallel correlated conductivity. The top figure shows the gates from -1.5 to 0.0 while the bottom figure shows the gates from 0.0 to 2.0. The numbers on the graphs is the gate energy. The y-axis is in units of $\frac{e^2}{\hbar}$

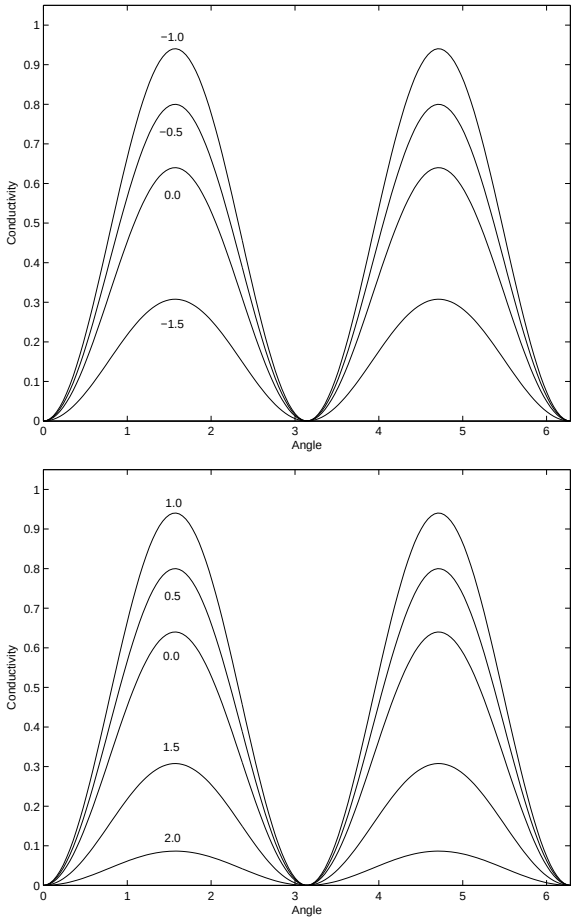

Figure 7.9: The gate dependence of the anti-parallel coherent conductivity. The top figure shows the gates from -1.5 to0.0 while the bottom figure shows the gates from 0.0 to 2.0. The numbers on the graphs is the gate energy. The y-axis is in units of $\frac{e^2}{\hbar}$

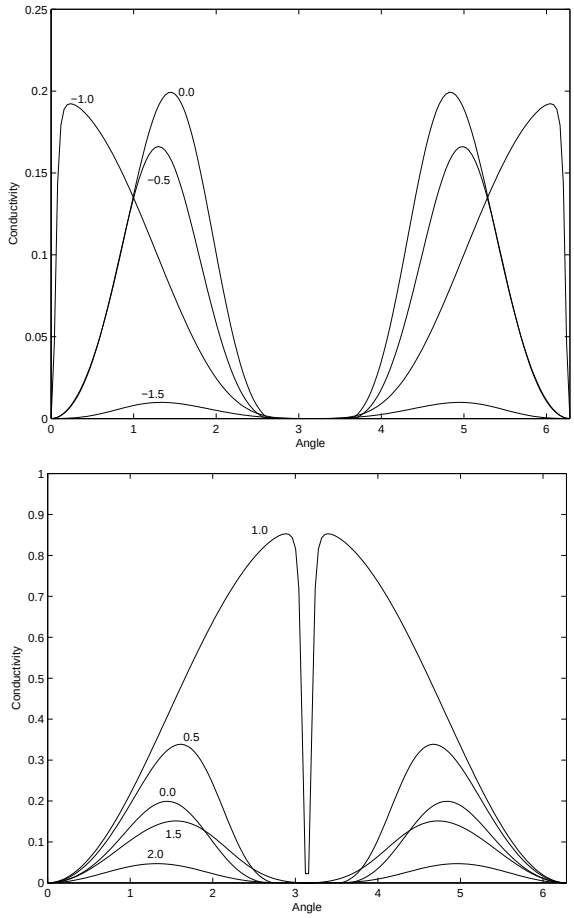

Figure 7.10: The gate dependence of the anti-parallel correlated conductivity. The top figure shows the gates from $-1.5 to 0.0$ while the bottom figure shows the gates from 0.0 to 2.0. The numbers on the graphs is the gate energy. The y-axis is in units of $\frac{e^2}{\hbar}$

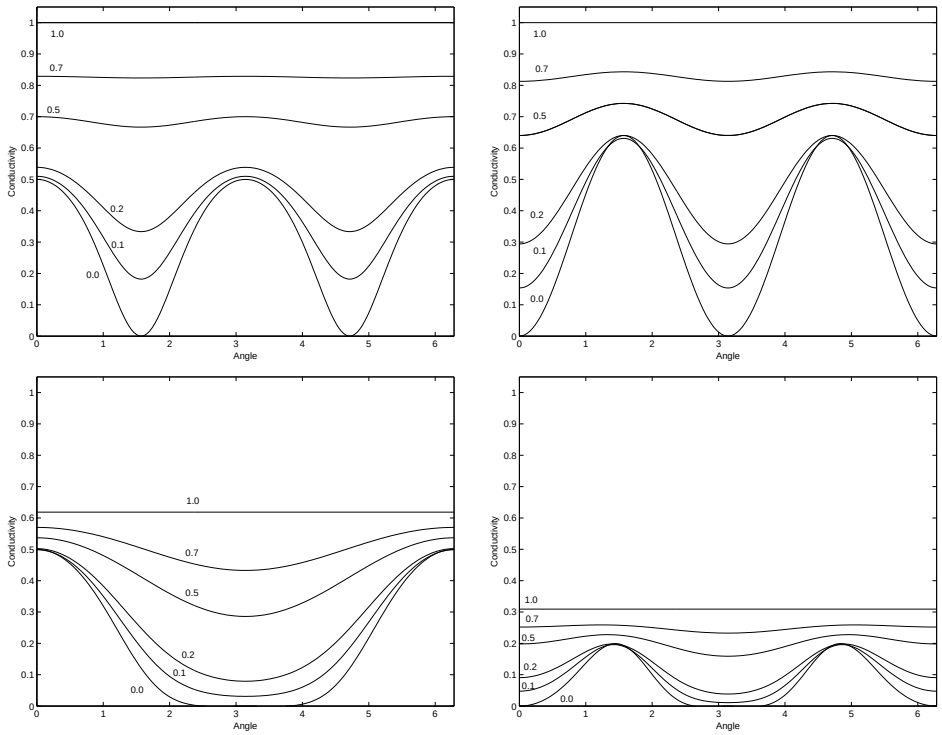

Figure 7.11: Graphs showing how the conductivities depend on the polarization of the leads. The numbers on the graphs show the polarization. The top left is the parallel coherent conductivity, the bottom left is the parallel correlated conductivity, the top right is the anti-parallel coherent conductivity and the bottom right is the anti-parallel correlated conductivity.

that the anti-parallel configuration has not preferred direction. Hence the shifts of the peaks are very difficult to predict. The up level of the dot has the lowest energy. Hence most of the transport will pass through this level. This explains how the conductivity increases as the up level moves toward the Fermi energy. This is because an electron in the dot will increase its probability to tunnel out as the level gets closer to the Fermi level.

The dependence on the polarization of the leads

In figure 7.11 the conductivities with finite polarizations are shown. It is seen that the current increases and the different effects decrease as the polarization increases. This is because, it is no longer only particles with one kind of spin which moves through the system. The increased current is because of spin valve effect losses its importance. Furthermore, we can see that the interference only works when there is no electrons with opposite spin which takes part in the current.

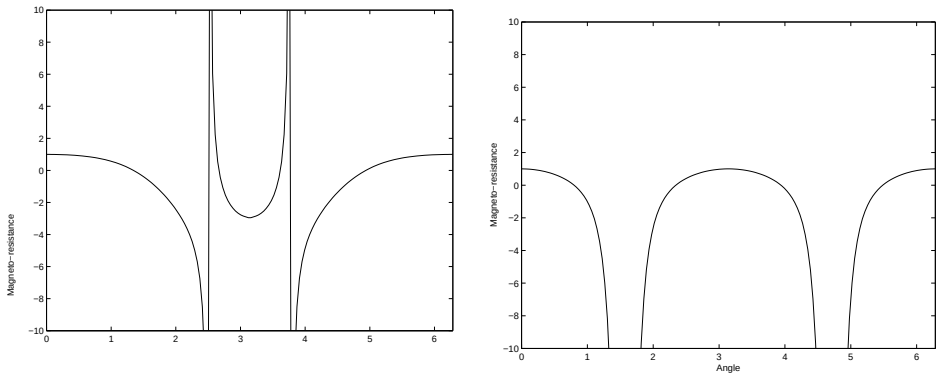

Figure 7.12: The two figures show the magneto-resistance for correlated regime (left) and the coherent regime (right). The level energies are positioned symmetric around the Fermi level.

7.5.3 Magneto-resistance

When comparing the current through a system with a parallel configuration with a system with an anti-parallel configuration it is useful to obtain the quantity called the magneto-resistance. The magneto-resistance is defined as

$$MR = \frac{J_P - J_{AP}}{J_P} = 1 - \frac{J_{AP}}{J_P} \tag{7.15}$$

This is the relative (and therefore dimensionless) difference between the parallel and anti-parallel currents.

Considering the coherent results, the quotient on the right hand side is proportional to $a^2 \tan(\theta)$. Therefore in an interval around $\theta = \frac{\pi}{2}$ the magneto-resistance is negative. This means that the anti-parallel current is greater than the parallel. This is solely due to the interference effect discussed earlier.

The same can happen in the correlated transport regime. Here it is due to the strong Coulomb effect instead of the interference effect

CHAPTER 8

Summary and outlook

The aim of the thesis was to uncover how the electric current and the spin torque is behaving in a system where a current is running through a quantum dot connected to magnetic contacts. An understanding of the current behavior in such a system is urgently needed to give an explanation of resent experiments.

8.1 General trace formula

A theoretical model inspired by the works of Jauho et.al. [12], Meir et.al. [24], Sergueev et.al. [33] and Waintal et.al. [36] was build. The model assumes a spin splitting of the quantum dot due to an external magnetic field. Therefore the spin variables were separated from the other variables and treated in their own Hilbert space. The model can deal with arbitrary directions of the magnetizations of the contacts and the quantum dot. The electric current and the spin torque was calculated using non-equilibrium Green's functions. The derivations led to the general trace formula for the current (4.14) and for the spin torque (4.17). These formulas have the form of an energy integral over a trace of a two-by-two matrix times the difference of the Fermi functions of the contacts. The two-by-two matrix contains information of the tunnelling-in and tunnelling-out processes involved. This information is expressed in terms of the quantum dot Green's function.

Two models were made for the quantum dot. The first rather simple one was the non-interacting dot formula. Here no internal interactions take place in the dot and the model was solved excatly. This model is used to describe the coherent transport regime.

The other model was the constant Coulomb interaction model. This model was solved in the strong Coulomb limit and is used to describe strongly correlated transport.

8.2 Current

The current was calculated in two configurations of the magnetizations in both the coherent and correlated regimes. This was done in the linear response approximation. In The first configuration the magnetizations of the contacts are parallel and the quantum dot magnetization has an angle to the parallel direction. The second configuration is the same except that the contact magnetizations are anti-parallel instead of parallel.

The most surprising result was the zero resonance in the coherent transport regime in the parallel configuration. This resonance appeared due to interference between the paths through the quantum dot and is robust to the tunnelling self-energy. The resonance is destroyed in the strong Coulomb limit. This is because the strong Coulomb interaction close the transport through one of the levels of the quantum dot.

The currents in all the configurations show a spin valve effect. This is due to the different magnetizations of the regions. The effect decreases when the polarization of the leads tends towards unity, i.e.for non-magnetized metals. The spin valve effect together with the coherent resonance can in some cases lead to a negative magneto-resistance. This means that the current is larger in the anti-parallel configuration than in the parallel configuration. This can also occur when the spin valve and the strong Coulomb effects are combined.

8.3 Outlook

There are several ways this work can be extended. Most importantly, however, it should be tested how well it can be used to explain the effects recently observed in experiments [13].

Furthermore this work could be extended to include the transition between the coherent transport and strongly correlated transport regimes. This could be achieved by solving the Coulomb model instead of taking the strong Coulomb limit. This would probably show that the Coulomb interaction slowly turns of the coherent resonance.

The spin torque formulas were not closely examined here because of the time limitations. Therefore this subject remains open for future studies.

Finally the general trace formula were derived without the specific need that the region between the leads is a quantum dot. Therefore the result could be used to examine spin-polarized transport through different systems as well.

APPENDIX A

List and definition of symbols

$\vec{a}_k^{(\dagger)} = \begin{pmatrix} a_{k\uparrow}^{(\dagger)} \\ ma_{k\downarrow}^{(\dagger)} \end{pmatrix}$: Spinnor creation operator

$\bar{A}$: Spin space matrix
$\mathbf{A}$: Quantum dot space matrix

$\mathrm{Tr}_s[\bar{N}_i] = \sum_\mu N_{i,\mu\mu}$: Trace in spin space

$\mathrm{Tr}_n[\mathbf{N}] = \sum_n N_{n,n}$: Trace in quantum dot space

$\sigma_x, \sigma_y, \sigma_z$: Pauli spin matrices $\begin{bmatrix} 0 & 1 \\ 1 & 0 \end{bmatrix}, \begin{bmatrix} 0 & -i \\ i & 0 \end{bmatrix}, \begin{bmatrix} 1 & 0 \\ 0 & -1 \end{bmatrix}$.
σ_i : Spin-occupation matrices ($i = 0, 1, 2, 3$)
σ, μ, ν, η : Spin indices
$\bar{\mu}$: The opposite spin of μ
k, q : Lead quantum numbers
n, m : Middle region / quantum dot quantum numbers
α, β : Lead region
ρ : Region (leads or middle region)

$V^*_{n\sigma,k\alpha\eta} = (V_{k\alpha\eta,n\sigma})^*$: Hermitian conjugate matrix in indices notation

$\otimes$: Matrix product

$\bar{\mathbf{\Gamma}}^\alpha$: The line width function for the α lead.
$\bar{\mathbf{\Gamma}}$: The sum of the line width functions for the leads.

$\bar{\mathbf{\Sigma}}_0^a$: Advanced self-energy for the tunnelling processes .
$\bar{\mathbf{\Sigma}}^a$: Advanced self-energy including both the tunnelling and Coulomb processes.
$\bar{\mathbf{\Sigma}}_0^r$: Retarded self-energy for the tunnelling processes .
$\bar{\mathbf{\Sigma}}^r$: Retarded self-energy including both the tunnelling and Coulomb processes.
$\bar{\mathbf{\Sigma}} = \bar{\mathbf{\Sigma}}^r - \bar{\mathbf{\Sigma}}^a$: Difference of the retarded and advanced self-energies.
$\bar{\mathbf{\Sigma}}_0 = \bar{\mathbf{\Sigma}}_0^r - \bar{\mathbf{\Sigma}}_0^a$: Difference of the retarded and advanced tunnelling self-energies.

APPENDIX B

Definitions and calculations

B.1 Commutator - anti commutator

In the text different commutation and anti-commutation rules are used extensively. They are presented in this section of the appendix.

The commutator between two operators are defined as

$$[A, B] = AB - BA \tag{B.1}$$

The anticommutator between two operators are defined as

$$\{A, B\} = AB + BA \tag{B.2}$$

For arbitrary operators the following general rules apply

$$\begin{aligned} [A; B] &= -[B; A] \\ \{A; B\} &= \{B; A\} \\ [AB; C] &= A[B; C] + [A; C]B \\ [AB; C] &= A\{B; C\} - \{A; C\}B \end{aligned} \tag{B.3}$$

B.1.1 The fermion algebra and relations

The operator algebra for the fermionic creation and annihilation operators are defined as

$$\begin{aligned} \{d_\eta; d_\nu\} &= \{d_\eta^\dagger, d_\nu^\dagger\} = 0 \\ \{d_\eta; d_\nu^\dagger\} &= \delta_{\eta\nu} \end{aligned} \tag{B.4}$$

By applying the algebraic and general rules the following commutator ralations can be derived:

$$[d^\dagger_\nu d_{\nu'}; d_\eta] = -d_{\nu'}\delta_{\nu\eta} \tag{B.5}$$

$$[d^\dagger_\nu d_{\nu'}, d^\dagger_\eta] = d^\dagger_\nu \delta_{\nu'\eta} \tag{B.6}$$

$$[d^\dagger_\nu d_{\nu'}; d^\dagger_\eta d_{\eta'}] = d^\dagger_\nu d_{\eta'}\delta_{\nu'\eta} - d^\dagger_\eta d_{\nu'}\delta_{\nu\eta'} \tag{B.7}$$

$$[d^\dagger_\nu d_{\nu'} d^\dagger_\eta d_{\eta'}; d_\sigma] = -d^\dagger_\nu d_{\nu'} d_{\eta'}\delta_{\eta\sigma} - d_{\nu'} d^\dagger_\eta d_{\eta'}\delta_{\nu\sigma} \tag{B.8}$$

$$[d^\dagger_\nu d_{\nu'}; d^\dagger_\eta d_{\eta'} d_\sigma] = d^\dagger_\nu d_{\eta'} d_\sigma \delta_{\eta\nu'} - d^\dagger_\eta d_{\eta'} d_{\nu'}\delta_{\nu\sigma} - d^\dagger_\eta d_{\nu'} d_\sigma \delta_{\nu\eta'} \tag{B.9}$$

$$\begin{aligned}[d^\dagger_\nu d_\nu d^\dagger_\mu d_\mu; d^\dagger_\eta d_{\eta'}] =& d^\dagger_\nu d_\nu \left(d^\dagger_\mu d_{\eta'}\delta_{\mu\eta} - d^\dagger_\eta d_\mu \delta_{\mu\eta'}\right) \\ &+ \left(d^\dagger_\nu d_{\eta'}\delta_{\nu\eta} - d^\dagger_\eta d_\nu \delta_{\nu\eta'}\right) d^\dagger_\mu d_\mu = 0\end{aligned} \tag{B.10}$$

$$\begin{aligned}[d^\dagger_\nu d_{\nu'} d^\dagger_\sigma d_{\sigma'}; d^\dagger_\eta d_{\eta'} d_\gamma] =& d^\dagger_\nu d_{\nu'} d^\dagger_\sigma d_{\eta'} d_\gamma \delta_{\eta\sigma'} - d^\dagger_\nu d_{\nu'} d^\dagger_\eta d_{\eta'} d_{\sigma'}\delta_{\sigma\gamma} - d^\dagger_\nu d_{\nu'} d^\dagger_\eta d_{\sigma'} d_\gamma \delta_{\sigma\eta'} \\ &+ d^\dagger_\nu d_{\eta'} d_\gamma d^\dagger_\sigma d_{\sigma'}\delta_{\eta\nu'} - d^\dagger_\eta d_{\eta'} d_{\nu'} d^\dagger_\sigma d_{\sigma'}\delta_{\nu\gamma} - d^\dagger_\eta d_{\nu'} d_\gamma d^\dagger_\sigma d_{\sigma'}\delta_{\eta',\nu}\end{aligned} \tag{B.11}$$

B.2 B^r-Green's function calculations

The calculations needed to find the EOM equations for the B-functions in section 6.2.2 are presented here. Due to the similarity of the calculations in section 6.2.2 only a few comments are presented.

B.2.1 $B^{r,1}$-EOM

$$i\partial_t B^{r,1}_{k\alpha\sigma m\mu,n\nu}(t-t') = \delta(t-t')\left\langle \left\{ a^\dagger_{k\alpha\sigma} d_{\bar\mu} d_\mu(t); d^\dagger_\nu(t')\right\}\right\rangle \tag{B.12}$$

The expectation of the anti-commutator is calculated sepeartely for the diagonal and antidiagonal terms.

Diagonal $\mu = \nu$

$$\left\langle \left\{ a^\dagger_{k\alpha\sigma} d_{\bar\mu} d_\mu(t); d^\dagger_\mu(t')\right\}\right\rangle \delta(t-t') = \left\langle a^\dagger_{k\alpha\sigma} d_{\bar\mu}\right\rangle \tag{B.13}$$

Antidiagonal $\mu \neq \nu$

$$\left\langle \left\{ a^\dagger_{k\alpha\sigma} d_{\bar\mu} d_\mu(t); d^\dagger_{\bar\mu}(t')\right\}\right\rangle \delta(t-t') = \left\langle a^\dagger_{k\alpha\sigma} d_{\bar\mu}\right\rangle \tag{B.14}$$

The time derivative in the anti-commutator

$$i\partial_t \left(a^\dagger_{k\alpha\sigma} d_{\bar\mu} d_\mu(t)\right) = -[H_0^{lead} + H_0^{QD} + H_T + H_{Coul}; a^\dagger_{k\alpha\sigma} d_{\bar\mu} d_\mu](t) \tag{B.15}$$

The lead term

$$[H_0^{lead}; a^\dagger_{k\alpha\sigma} d_{\bar\mu} d_\mu] = \epsilon_{k\alpha\sigma} a^\dagger_{k\alpha\sigma} d_{\bar\mu} d_\mu \tag{B.16}$$

The quantum dot term

$$[H_0^{QD}; a^\dagger_{k\alpha\sigma} d_{\bar{\mu}} d_\mu] = -\left(\epsilon_\mu + \epsilon_{\bar{\mu}}\right) a^\dagger_{k\alpha\sigma} d_{\bar{\mu}} d_\mu \tag{B.17}$$

The Coulomb term

$$\begin{aligned}[H_{Coul}; a^\dagger_{k\alpha\sigma} d_{\bar{\mu}} d_\mu] = & \\ & -\frac{U}{2}\Big(n_{\bar{\mu}} a^\dagger_{k\alpha\sigma} d_{\bar{\mu}} d_\mu + n_\mu a^\dagger_{k\alpha\sigma} d_{\bar{\mu}} d_\mu \\ & \qquad + a^\dagger_{k\alpha\sigma} d_{\bar{\mu}} d_\mu n_{\bar{\mu}} + a^\dagger_{k\alpha\sigma} d_{\bar{\mu}} d_\mu n_\mu \Big) \\ & = -U a^\dagger_{k\alpha\sigma} d_{\bar{\mu}} d_\mu \end{aligned} \tag{B.18}$$

The tunnelling term

$$\begin{aligned}[H_T; a^\dagger_{k\alpha\sigma} d_{\bar{\mu}} d_\mu] = & \sum_\eta V^*_{\eta,k\alpha\sigma} d^\dagger_\eta d_{\bar{\mu}} d_\mu \\ & + \sum_{q\beta\sigma'} \left(V^*_{\mu,q\beta\sigma'} a^\dagger_{k\alpha\sigma} a_{q\beta\sigma'} d_{\bar{\mu}} - V^*_{\bar{\mu},q\beta\sigma'} a^\dagger_{k\alpha\sigma} a_{q\beta\sigma'} d_\mu \right) \end{aligned} \tag{B.19}$$

Using the decoupling and Hartree-Fock approximation in section 6.2.3) gives the following equation of motion for B^1

$$\begin{aligned} & \Big(\omega - \big(\epsilon_\mu + \epsilon_{\bar{\mu}}\big) + \epsilon_{k\alpha\sigma} - U\Big) B^{r,1}_{k\alpha\sigma\mu,\nu}(\omega) = \\ & \quad \sum_\eta V^*_{\eta,k\alpha\sigma} C^r_{\eta\bar{\mu}\mu,\nu}(\omega) + V^*_{\bar{\mu},k\alpha\sigma} n_{k\alpha\sigma} D^r_{\mu,\nu} - V^*_{\mu,k\alpha\sigma} n_{k\alpha\sigma} D^r_{\bar{\mu},\nu} \end{aligned} \tag{B.20}$$

B.2.2 $B^{r,2}$-EOM

$$\begin{aligned} i\partial_t B^{r,2}_{\mu k\alpha\sigma,\nu}(t-t') = & \delta(t-t') \left\langle \left\{ d^\dagger_{\bar{\mu}} d_\mu a_{k\alpha\sigma}(t); d^\dagger_\nu(t') \right\} \right\rangle \\ & + (-i)\theta(t-t') \left\langle \left\{ i\partial_t \left(d^\dagger_{\bar{\mu}} d_\mu a_{k\alpha\sigma}(t) \right); d^\dagger_\nu(t') \right\} \right\rangle \end{aligned} \tag{B.21}$$

The diagonal and antidiagonal terms of the expectation of the anti-commutator are calculated seperately.

Diagonal $\mu = \nu$

$$\left\langle \left\{ d^\dagger_{\bar{\mu}} d_\mu a_{k\alpha\sigma}(t); d^\dagger_\mu(t') \right\} \right\rangle \delta(t-t') = \left\langle d^\dagger_{\bar{\mu}} a_{k\alpha\sigma} \right\rangle \tag{B.22}$$

Antidiagonal $\mu \neq \nu$

$$\left\langle \left\{ d^\dagger_{\bar{\mu}} d_\mu a_{k\alpha\sigma}(t); d^\dagger_{\bar{\mu}}(t') \right\} \right\rangle \delta(t-t') = 0 \tag{B.23}$$

The time derivative in the anti-commutator

$$i\partial_t \left(d^\dagger_{\bar{\mu}} d_\mu a_{k\alpha\sigma}(t) \right) = -[H_0^{lead} + H_0^{QD} + H_T + H_{Coul}; d^\dagger_{\bar{\mu}} d_\mu a_{k\alpha\sigma}](t) \quad \text{(B.24)}$$

The lead term

$$[H_0^{lead}; d^\dagger_{\bar{\mu}} d_\mu a_{k\alpha\sigma}] = -\epsilon_{k\alpha\sigma} d^\dagger_{\bar{\mu}} d_\mu a_{k\alpha\sigma} \quad \text{(B.25)}$$

The quantum dot term

$$[H_0^{QD}; d^\dagger_{\bar{\mu}} d_\mu a_{k\alpha\sigma}] = -\left(\epsilon_\mu - \epsilon_{\bar{\mu}}\right) d^\dagger_{\bar{\mu}} d_\mu a_{k\alpha\sigma} \quad \text{(B.26)}$$

The Coulomb term

$$\begin{aligned} [H_{Coul}; d^\dagger_{\bar{\mu}} d_\mu a_{k\alpha\sigma}] = & \\ & -\frac{U}{2}\Big(n_\mu d^\dagger_{\bar{\mu}} d_\mu a_{k\alpha\sigma} - n_{\bar{\mu}} d^\dagger_{\bar{\mu}} d_\mu a_{k\alpha\sigma} \\ & \qquad + d^\dagger_{\bar{\mu}} d_\mu a_{k\alpha\sigma} n_{\bar{\mu}} - d^\dagger_{\bar{\mu}} d_\mu a_{k\alpha\sigma} n_\mu \Big) \\ & = -U d^\dagger_{\bar{\mu}} d_\mu a_{k\alpha\sigma} \end{aligned} \quad \text{(B.27)}$$

The tunnelling term

$$\begin{aligned} [H_T; d^\dagger_{\bar{\mu}} d_\mu a_{k\alpha\sigma}] = & -\sum_\eta V_{k\alpha\sigma,\eta} d^\dagger_{\bar{\mu}} d_\mu d_\eta \\ & - V_{q\beta\sigma',\bar{\mu}} a^\dagger_{q\beta\sigma'} a_{k\alpha\sigma} d_\mu - V^*_{\mu,q\beta\sigma'} d^\dagger_{\bar{\mu}} a_{q\beta\sigma'} a_{k\alpha\sigma} \end{aligned} \quad \text{(B.28)}$$

Using the decoupling and Hartree-Fock approximation in section 6.2.3 gives the following equation of motion for B^2

$$\begin{aligned} \left(\omega - (\epsilon_\mu - \epsilon_{\bar{\mu}}) - \epsilon_{k\alpha\sigma} - U\right) B^{r,2}_{k\alpha\sigma\mu,\nu}(\omega) = & \\ \sum_\eta V^*_{\eta,k\alpha\sigma} C^r_{\eta\bar{\mu}\mu,\nu}(\omega) + V_{k\alpha\sigma,\bar{\mu}} n_{k\alpha\sigma} D^r_{\mu,\nu}(\omega) & \end{aligned} \quad \text{(B.29)}$$

$B^{r,3}$-EOM

$$\begin{aligned} i\partial_t B^{r,3}_{\bar{\mu}k\alpha\sigma,\nu}(t-t') = & \delta(t-t') \left\langle \left\{ n_{\bar{\mu}} a_{k\alpha\sigma}(t); d^\dagger_\nu(t') \right\} \right\rangle \\ & + (-i)\theta(t-t') \left\langle \left\{ i\partial_t \left(n_{\bar{\mu}} a_{k\alpha\sigma}(t) \right); d^\dagger_\nu(t') \right\} \right\rangle \end{aligned} \quad \text{(B.30)}$$

The diagonal and antidiagonal terms of the expectation of the anti-commutator are calculated seperately.

Diagonal $\mu = \nu$

$$\left\langle \left\{ n_{\bar{\mu}} a_{k\alpha\sigma}(t); d^\dagger_\mu(t') \right\} \right\rangle \delta(t-t') = 0 \quad \text{(B.31)}$$

Antidiagonal $\mu \neq \nu$

$$\left\langle \left\{ n_{\bar{\mu}} a_{k\alpha\sigma}(t); d^{\dagger}_{\bar{\mu}}(t') \right\} \right\rangle \delta(t-t') = \langle d_{\bar{\mu}} a_{k\alpha\sigma} \rangle \tag{B.32}$$

The time derivative in the anti-commutator

$$i\partial_t \left(n_{\mu} a_{k\alpha\sigma}(t) \right) = -[H_0^{lead} + H_0^{QD} + H_T + H_{Coul}; d^{\dagger}_{l\eta} d_{m\mu} a_{k\alpha\sigma}](t) \tag{B.33}$$

The lead term

$$[H_0^{lead}; n_{\bar{\mu}} a_{k\alpha\sigma}] = -\epsilon_{k\alpha\sigma} n_{\bar{\mu}} a_{k\alpha\sigma} \tag{B.34}$$

The quantum dot term

$$[H_0^{QD}; n_{\bar{\mu}} a_{k\alpha\sigma}] = -\left(\epsilon_{m\mu} - \epsilon_{l\eta} \right) n_{\bar{\mu}} a_{k\alpha\sigma} \tag{B.35}$$

The Coulomb term

$$[H_{Coul}; n_{\bar{\mu}} a_{k\alpha\sigma}] = \sum_{\epsilon t a} [n_{\bar{\eta}} n_{\eta}; n_{\bar{\mu}} a_{k\alpha\sigma}] = 0 \tag{B.36}$$

The tunnelling term

$$\begin{aligned} [H_T; n_{\bar{\mu}} a_{k\alpha\sigma}] = &- \sum_{\eta} V_{k\alpha\sigma,\eta} n_{\mu'} d_{\eta} \\ &- \sum_{q\beta\sigma'} \left(V^{*}_{\bar{\mu},q\beta\sigma'} d^{\dagger}_{\bar{\mu}} a_{q\beta\sigma'} a_{k\alpha\sigma} + V_{q\beta\sigma',\bar{\mu}} a^{\dagger}_{q\beta\sigma'} a_{k\alpha\sigma} d_{\bar{\mu}} \right) \end{aligned} \tag{B.37}$$

Using the decoupling and Hartree-Fock approximation in section 6.2.3 gives the following equation of motion for B^3

$$\left(\omega - \epsilon_{k\alpha\sigma} \right) B^{r,3}_{\mu k\alpha\sigma,\nu}(\omega) = \sum_{\eta} V_{k\alpha\sigma,\eta} C^{r}_{\bar{\mu}\bar{\mu}\eta,\nu}(\omega) + V_{k\alpha\sigma,\bar{\mu}} a^{\dagger}_{k\alpha\sigma} a_{k\alpha\sigma} D^{r}_{\bar{\mu},\nu} \tag{B.38}$$

B.3 Identities used in time integration

The following identities is used in the calculation of the time integral in section 4.2.

$$\begin{aligned} \left(\bar{\mathbf{\Gamma}}^{\alpha}(\epsilon) \right)^{*} &= 2\pi \sum_{\gamma} \rho(\epsilon)^{*} \left(\bar{V}^{\dagger}_{\gamma}(\epsilon) \right)^{*} \left(\bar{V}_{\gamma}(\epsilon) \right)^{*} \\ &= 2\pi \sum_{\gamma} \rho(\epsilon) \left(\bar{V}^{\dagger}_{\gamma}(\epsilon) \bar{V}_{\gamma}(\epsilon) \right)^{t} = \left(\bar{\mathbf{\Gamma}}^{\alpha}(\epsilon) \right)^{t} \end{aligned} \tag{B.39}$$

$$\bar{\sigma}^{*} = (\sigma_x, -\sigma_y, \sigma_z) = \bar{\sigma}^{t} \tag{B.40}$$

$$\left(\bar{D}^{r}_{m\mu n\nu}(\omega - ic) \right)^{*} = \left(\bar{D}^{a}_{m\mu n\nu}(\omega + ic) \right)^{t} \tag{B.41}$$

$$\begin{aligned}\left(\bar{D}^{<}_{m\mu n\nu}(\omega - ic)\right)^{*} &= \left(\int \frac{d\omega}{2\pi} \exp\left(i(\omega - ic)(t - t')\right)(-i) \left\langle d^{\dagger}_{m\mu}(t') d_{n\nu}(t) \right\rangle\right) \\ &= -\int \frac{d\omega}{2\pi} \exp\left(i(\omega - ic)(t' - t)\right)(-i) \left\langle d^{\dagger}_{n\nu}(t) d_{m\mu}(t') \right\rangle \\ &= -\left(\bar{D}^{<}_{n\nu m\mu}(\omega + ic)\right)\end{aligned} \tag{B.42}$$

Bibliography

[1] I.L. Aleiner, P.W Brouwer, and L.I. Glazman. Quantum effects in coulomb blockade. *Physics Reports*, 358(5-6), March 2002.

[2] P. W. Anderson. Localized magnetic states in metals. *Physical Review*, 124(1), 1961.

[3] C.W.J. Beenakker. Theory of Coulomb-blockade oscillations in the conductance of a quantum dot. *Physical Review B*, 44:1646, 1991.

[4] H. Bruus and K. Flensberg. *Introduction to Quantum field theory in condensed matter physics.* Ørsted Laboratory, Niels Bohr Institute, Copenhagen, 2001.

[5] S. Datta and B. Das. Electronic analog of the electro-optic modulator. *Applied Physics Letters*, 56(665), February 1990.

[6] J.H. Davies. *The Physics of Low-Dimentional Semiconductors.* Cambridge University Press, 1998.

[7] D. K. Ferry and S. M. Goodnick. *Transport in Nanostructures*, volume 6 of *Cambridge Studies in Semiconductor Physics and Microelectronic Engineering.* Cambridge Univercity Press, Cambridge, 1997.

[8] R. Fiederling, M. Keim, G. Reuscher, W. Ossau, G. Schmidt, A. Waag, and L.W. Molenkamp. Injection and detection of a spin-polarized current in a light-emitting diode. *Nature*, 402:787, December 1999.

[9] A.T. Hanbicki, B.T. Jonker, G. Itskos, G. Kioseoglou, and A. Petrou. Efficient electrical spin injection from a magnetic metal/tunnel barrier contact into a semiconductor. *Applied Physic Letters*, 80:1240, February 2002.

[10] H. Haug and A.-P. Jauho. *Quantum Kinetics in Transport and Optics of Semiconductors*. Springer Series in Solid-State Sciences 123. Springer-Verlag, Berlin Heidelberg, 1996.

[11] X. Hoffer, C. Klinke, J.-M. Bonard, L. Gravier, and J.-E. Wegrowe. Spin-dependent magnetoresistance and spin-charge separation in multi-wall carbon nanotubes. *cond-mat/*, (0303314 v2), 2003.

[12] A.-P. Jauho, N.S. Wingreen, and Y. Meir. Time-dependent transport in interacting and noninteracting resonant-tunneling systems. *Physical Review B*, 50(8):5528, 1994.

[13] A. Jensen. *Ferromagnetically Contacted Single-Wall Carbon Nanotubes*. PhD thesis, Nano-Science Center, Ørsted Lab. NBIfAPG, University of Copenhagen, July 2003.

[14] M. Johnson and R.H. Silsbee. Interfacial charge-spin coupling: Injection and detection of spin magnetization in metals. *Physical Review Letters*, 55(1790):225, October 1985.

[15] M. Julliére. Tunneling between ferromagnetic films. *Physical Letters A*, 54:225, 1975.

[16] L.P. Kadanoff and G. Baym. *Quantum Statistical Mechanics*. Benjamin, New York, 1962.

[17] L.V. Keldysh. *Zh. Eksp. Teor. Fiz.*, 47:1515 [Sov. Phys. JETP 20, 20, 1018 (1965)], 1964.

[18] J. König and J. Martinek. Interaction-driven spin precession in quantum-dot spin valves. *cond-mat/0212253*, 2002.

[19] L.D. Landau and E.M. Lifshitz. *Quantum Mechanics*, volume 3 of *Course of Theoretical Physics,*. Butterworth-Heinemann, Oxford, third edition edition, 1998.

[20] D. C. Langreth. *Linear and Nonlinear Electron Transport in Solids*, volume 17 of *NATO Advanced Study Institutes Series*, chapter 1, pages 3–32. Plenum Press, New York, 1976.

[21] G.D. Mahan. *Many-Particle Physics*. Physics of Solids and Liquids. Kluwer Academic / Plenum Publishers, New York, third edition edition, 2000.

[22] P.C. Martin and J. Schwinger. *Physical Review*, 115:1342, 1959.

[23] Y. Meir. Landauer formula for the current through an interacting electron region. *Physical Review Letters*, 68(16):2512, April 1992.

[24] Y. Meir, N.S. Wingreen, and P.A. Lee. Transport through a strongly interacting electron system: Theory of periodic conductance oscillations. *Physical Review Letters*, 66(23):3048, 1991.

[25] U. Meirav, M.A. Kastner, and S.J. Wind. Single-electron charging and period coductance resonances in GaAs nanostructures. *Physical Review Letters*, 65(6):771, August 1990.

[26] E. Merzbacher. *Quantum Mechanics*. John Wiley and Sons, Inc., 3 edition, 1998.

[27] J.U. Nöckel and A.D. Stone. Resonance line shapes in quasi-onedimentional scattering. *Physical Review B*, 50(23):17415, December 1994.

[28] T.-K. Ng. ac response in the nonequilibrium Anderson impurity model. *Physical Review Letters*, 76:487, 1996.

[29] Y. Ohno, D.K. Young, B. Beschoten, F. Matsukura, H. Ohno, and D.D. Awschalom. Electrical spin injection in a ferromagnetic semiconductor heterostructure. *Nature*, 402:790, December.

[30] R.M. Potok, J.A. Folk, C.M. Marcus, V. Umansky, M. Hanson, and A.C. Gossard. Spin and Polarized Current from Coulomb Blockaded Quantum Dots. *Physical Review Letters*, 91:016802, July 2003.

[31] J. Rammer and H. Smith. Quantum field-theoretical methods in transport theory of metals. *Rewiews of Modern Physics*, 58(2), 1986.

[32] J. Schwinger. *Journal of Mathematical Physics (N.Y.)*, 2:407, 1961.

[33] N. Sergueev, Qing-feng Sun, Hong Guo, B. G. Wang, and Jian Wang. Spin-polarized transport through a quantum dot: Anderson model with on-site Coulomb repulsion. *Physical Rewiew B*, 65:165303, 2002.

[34] J.C. Slonczewski. Conductance and exchange coupling of two ferromagnets separated by a tunneling barrier. *Physical Review B*, 39(10):6995, April 1989.

[35] F. M. Souza, J. C. Egues, and A. P. Jauho. Current and noise in a fm/quantum dot/fm system. *cond-mat/0209263 v1*, Sep. 2002.

[36] X. Waintal, E.B. Myers, P. W. Brouwer, and D. C. Ralph. Role of spin-dependent interface scattering in generating current-induced torques in magnetic multilayers. *Physical Rewiew B*, 62(18):12 317, 2000.

[37] N.S. Wingreen, A.-P. Jauho, and Y. Meir. Time-dependent transport through a mesoscopic structure. *Physical Rewiew B*, 48:8487, 1993.

[38] P. Zhang, Q.-K. Xue, and X.C. Xie. Magnetoresistance of a mesoscopic tunneling quantum dot. *cond-mat/0201465 v1*, 2002.